



DEPARTMENT OF BIOLOGICAL AND
ENVIRONMENTAL SCIENCES

GENETIC REGULATION OF THE SHORT-TERM STOMATAL CO₂ RESPONSE IN *ARABIDOPSIS THALIANA*

NEETHU JOSEPH

Degree project for Master of Science (120 hec) with a major in Biology
BIO 727, Physiology and Cell biology (60hec)
Second cycle

Semester

/year: Spring 2024 – Spring 2025

Supervisors: Mats Andersson and Karin Johansson, Department of Biological
and Environmental Sciences

Examiner: Henrik Aronsson, Department of Biological and Environmental
Sciences

Contents

1	Introduction	3
1.1	Leaf gas exchange and the role of stomata	3
1.2	Regulation of stomatal movements.....	3
1.3	Stomatal behaviour under elevated CO ₂	4
1.4	Genetic regulation of stomatal responses to CO ₂	4
1.5	QTL mapping in MAGIC population	5
2	Aim and research objective	7
3	Materials and methods.....	7
3.1	Plant materials and growth conditions.....	7
3.2	Gas exchange measurements	8
3.3	Trait distribution and regression analysis.....	10
3.4	QTL mapping	11
3.5	Candidate gene analysis.....	12
3.6	Data cleaning and transformation	12
4	Result	13
4.1	Descriptive statistics of gas exchange traits	13
4.2	Correlation of different gas exchange traits	16
4.3	QTL mapping for gas exchange traits.....	18
4.4	QTL support interval	21
4.5	SNP association scan.....	22
4.6	Candidate Gene Analysis.....	24
4.6.1	SNP-Associated Gene	24
4.6.2	1.5-LOD Support Interval Linked Genes.....	24
5	Discussion.....	27
5.1	Next steps	29
6	Conclusion.....	30
	Acknowledgement	30
	References	31
	Appendix 1	40
	Popular science summary	40

Abstract

Plants respond to various environmental stimuli, including elevated CO₂, by partially closing their stomatal pores. This partial closure reduces water loss through transpiration while allowing photosynthesis to continue. Understanding how plants regulate this response is important for improving water use efficiency, especially in the context of climate change. However, the signalling pathways that control stomatal closure in response to CO₂ are complex, and many components are still unknown.

This study aimed to investigate the genetic basis of CO₂-induced stomatal closure in *Arabidopsis thaliana* using a Multiparent Advanced Generation Inter-Cross (MAGIC) population based on 19 founder lines. Gas exchange measurements were taken in 206 RILs, and quantitative trait locus (QTL) mapping was used to identify the genome regions linked to stomatal response to elevated CO₂ and related traits. A significant QTL was found on chromosome 1 associated with the percentage reduction in stomatal conductance in response to elevated CO₂. Further analysis of the genes in this region revealed 15 potential candidates. Additionally, a QTL on the same chromosome was linked to the speed of the response when CO₂ concentrations increased from 420 to 800 ppm.

This study provides a foundation for exploring these QTLs and candidate genes, with the potential to improve plant adaptation to increased CO₂ and enhance water-use efficiency in future climates.

Keywords: stomatal conductance, CO₂, *Arabidopsis thaliana*, MAGIC population, quantitative trait loci

1 Introduction

1.1 Leaf gas exchange and the role of stomata

Leaf gas exchange is vital for photosynthesis and water regulation in plants. It involves the uptake of carbon dioxide (CO_2) for photosynthesis and the release of water vapour (H_2O) and oxygen (O_2). Plants regulate leaf gas exchange by adjusting the turgor pressure of guard cells that surround the microscopic pores called stomata (Hetherington & Woodward, 2003; Kollist et al., 2014).

Stomatal conductance (g_s) quantifies the rate at which gases like CO_2 and water vapour pass through the stomata. It plays a significant role in plant growth, productivity, and environmental adaptation. The number, size, and aperture of stomata influence how efficiently plants regulate gas exchange and balance transpirational water loss. Higher stomatal conductance often correlates with improved crop yield because it enhances CO_2 uptake for photosynthesis, but this comes at the cost of increased water loss (Lu et al., 1998; Bahar et al., 2009; Prashar et al., 2013). Therefore, understanding how stomata function and adapt to environmental changes is increasingly important, particularly as rising atmospheric CO_2 levels influence plant behaviour, water use efficiency, and agricultural resilience.

1.2 Regulation of stomatal movements

A complex interaction of internal physiological mechanisms and external environmental signals regulates stomatal opening and closing. Environmental factors such as light intensity, humidity, soil water availability, and CO_2 influence stomatal behaviour (Driesen et al., 2020). Once guard cells sense environmental stimuli, they initiate a signalling network. Depending on the nature of the stimulus, the resulting pathway either increases or decreases the stomatal aperture. Stomatal regulation is achieved by changes in the turgor pressure of guard cells, driven by solute movement across the plasma membrane and vacuoles (Lawson & Blatt, 2014). Key solutes in this process include potassium (K^+), chloride (Cl^-), Nitrate ions (NO_3^-), malate²⁻ and sucrose. Stomatal opening starts when H^+ -ATPases pump protons out of the guard cells, causing membrane hyperpolarisation. This causes K^+ and other ions to enter the cells, lowering the water potential and increasing turgor pressure through osmosis. This pressure change causes the guard cells to expand, leading to

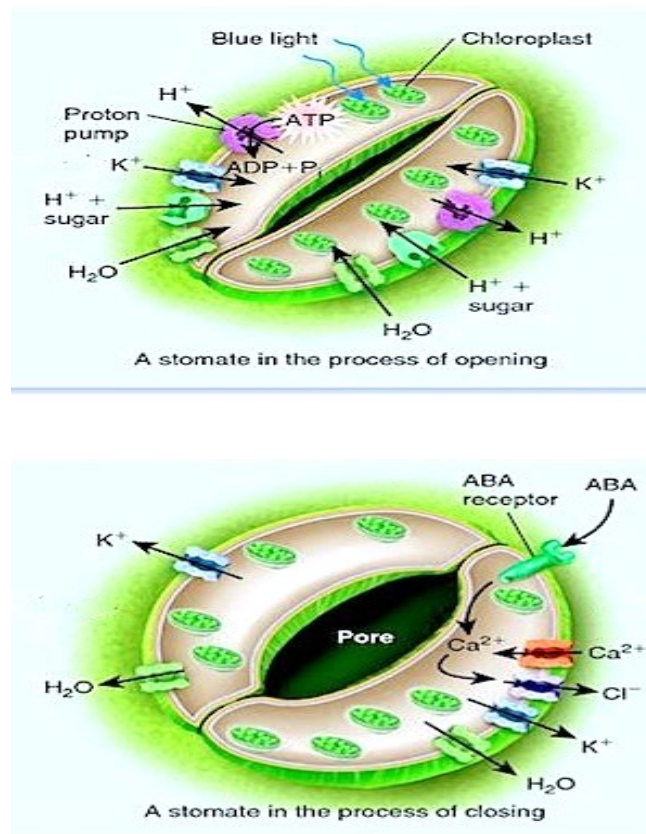


Figure 1. A basic model of ion fluxes regulating stomatal opening and closure. (<https://plantstomata.wordpress.com/2015/10/28/how-stomatal-pores-open-and-close/>)

stomatal pore opening (Figure 1) (Kim et al., 2010; Roux and Leonhardt., 2018). Stomatal closure can be triggered by environmental stresses, such as drought, pathogen attack and reduced air humidity. During closure, solutes are released from the guard cells, water exits by osmosis, and turgor pressure decreases, causing the guard cells to shrink and the stomatal pore to close (Kim et al., 2010).

1.3 Stomatal behaviour under elevated CO₂

Most plant species respond to elevated CO₂ levels by partial stomatal closure, leading to reduced stomatal conductance. This adjustment allows plants to take up sufficient CO₂ for photosynthesis while minimising transpirational water loss (Ainsworth and Rogers, 2007; Xu et al., 2016). The ability to regulate stomatal conductance in response to CO₂ is crucial because it affects their water economy and influences plant growth. However, the magnitude of this stomatal adjustment varies significantly among and within species, and is strongly influenced by environmental conditions, plant functional types, and developmental stages (Takahashi et al., 2015; Xu et al., 2016).

Reducing stomatal conductance under elevated CO₂ allows plants to maintain photosynthesis while using less water. Therefore, crops that respond well to elevated CO₂ may save water in future climates where water may be limited. Understanding how these responses work is essential for applying this knowledge in crop breeding or biotechnology. Identifying the key factors behind natural variation in short-term g_s responses could help select plant species with greater potential for improved water use efficiency under elevated CO₂ conditions.

Numerous studies have investigated stomatal responses to elevated CO₂. Short-term response is the change in stomatal conductance that occurs within minutes to hours when exposed to changes in CO₂. This involves rapid physiological adjustments, leading to partial stomatal closure (Morison, 1998; Haworth et al., 2013; Xu et al., 2016). The magnitude responses can vary greatly. For example, different *A. thaliana* accessions show a wide range of reactions, from 10% to 70% reduction in g_s , reflecting flexible stomatal behaviour under elevated CO₂ (Monda et al., 2016; Takahashi et al., 2015; Zinta et al., 2014). Long-term responses mean the change in stomatal conductance over weeks to months of exposure to elevated CO₂ concentration and involve structural changes like reduced stomatal density (Medlyn et al., 2001; Haworth et al., 2013). These longer-term adjustments also differ among plant types. For instance, angiosperms are more sensitive to elevated CO₂, exhibiting around 36 % reduction in stomatal conductance, whereas gymnosperms are far less sensitive, showing only a 3% reduction (Klein and Ramon, 2019). Although the link between short- and long-term responses is not fully understood, there is evidence that early stomatal behaviour may influence long-term adaptation patterns (Hasper et al., 2017; Johansson et al., 2020).

1.4 Genetic regulation of stomatal responses to CO₂

The molecular mechanisms behind the stomatal response to elevated CO₂ have been extensively studied in the model plant *A. thaliana*. Its small, rapid life cycle and ease of genetic manipulation make it an ideal model organism (Somerville & Koornneef, 2002). It is supported by extensive resources such as mapping populations, mutants, and databases containing gene function information. In addition, *A. thaliana* displays significant natural variation across accessions and shares many genes with economically important crop species, making it valuable

for translating findings to agriculture (Alonso-Blanco & Koornneef, 2000; Kover & Schaal, 2002; Ooka et al., 2003; Stracke et al., 2004).

Recent advances in genomics have revealed that stomatal regulation under elevated CO₂ is a complex trait controlled by multiple genes, each playing distinct roles in CO₂ sensing and signal transduction. Several genes have been identified as key regulators in this process. Also, numerous studies have shown that the CO₂ and abscisic acid pathways for stomatal closure merge at points downstream in the signalling cascade (Hsu et al., 2018). The signal transduction pathway begins when CO₂ enters the guard cells through the aquaporin PIP2 (Plasma Membrane Intrinsic Protein 2) channels or by simple transmembrane diffusion (Mori et al., 2014). Once inside, the carbonic anhydrases, such as β CA1 and β CA4 (Beta Carbonic Anhydrase 1 and 4), catalyse the conversion of CO₂ into bicarbonate (HCO₃⁻). This HCO₃⁻ acts as a secondary messenger, initiating the CO₂-induced stomatal closure pathway (Hu et al., 2010).

Bicarbonate has been shown to activate early signalling cascade components, most notably the MAPKs (Mitogen-Activated Protein Kinases), including MPK4 and MPK12. Recent studies have shown that MPK12 plays a key role in responding to high CO₂ levels and inhibiting HT1 (High Leaf Temperature 1) (Toldsepp et al., 2018; Takahashi et al., 2022). HT1 is a negative regulator of CO₂-induced stomatal closure (Hashimoto et al., 2006; H \ddot{o} rak et al., 2016). Once inhibited, HT1 allows the activation of downstream protein kinases such as OST1 (Open Stomata 1) or GHR1 (Guard Cell Hydrogen Peroxide-Resistant 1) (Sierla et al., 2018). OST1 is the converging component of the CO₂ and ABA-induced signal transduction pathway. These kinases subsequently activate the SLAC1 (Slow Anion Channel-Associated 1) anion channel, a key step in triggering ion efflux from the guard cells and initiating stomatal closure in response to elevated CO₂ levels (H \ddot{o} rak et al., 2016). Recently, the BIG protein in *A. thaliana* is also been identified to be involved in the CO₂-induced stomatal closure signal cascade (Hiyama et al., 2017; He et al., 2018). However, the precise interaction between these components has yet to be elucidated.

In addition to these molecular insights, a quantitative trait loci (QTL) mapping in *A. thaliana* identified a genetic locus involved in both short-term stomatal responses to CO₂ and long-term regulation of g_s under elevated CO₂ conditions, suggesting a possible genetic link between these responses (Johansson et al., 2020). While these discoveries have advanced our understanding, the complete mechanism of stomatal responses to elevated CO₂ remains unresolved. Further QTL mapping in *A. thaliana* Multi Parent Advanced Generation Inter-Cross (MAGIC) populations offers a promising path to identify additional genetic regulators.

1.5 QTL mapping in MAGIC population

Quantitative traits are measurable, continuously varying traits controlled by multiple genes (Falconer & Mackay, 1996; Holland, 2007). The chromosomal regions associated with these traits are known as Quantitative Trait Loci (QTLs). QTLs can be identified through a statistical approach known as QTL mapping, which links phenotypic variation with molecular marker data (Falconer & Mackay, 1996; Kearsey, 1998). This approach has been applied to map complex traits such as stomatal conductance in plants, providing insights into the genetic basis of quantitative traits (Huang et al., 2011).

Genetic mapping studies use genetically diverse populations to link genetic markers with phenotypic traits (Huang et al., 2011). The most common approaches are biparental mapping with populations like recombinant inbred lines (RILs), and Genome Wide Association Studies (GWAS) (Huang et al., 2009). Biparental populations are widely used for QTL mapping. They are stable lines generated by crossing two parent genotypes, normally with contrasting phenotypes for the trait of interest, and selfing or inbreeding for a number of generations to generate homozygous lines whose genomes are mosaics of the parental genotypes, which will show a range in phenotypes for the trait of interest. Once created and genotyped, they are easily reproducible and used for many different types of experiments (Scott et al., 2020). However, biparental populations have limited genetic diversity, as they only capture allelic variation from two parents. This results in lower mapping resolution due to fewer recombination events and a restricted number of allelic combinations (Huang et al., 2009; Xu et al., 2017).

On the other hand, GWAS is well-established and a common method to identify genomic regions associated with complex traits. They utilise a diverse collection of natural variation that captures broader genetic diversity. This generally leads to higher mapping resolution. However, GWAS can be affected by complex population structure, potentially leading to false associations if not carefully controlled (Myles et al., 2009; Vilhjálmsson & Nordborg, 2013; Korte & Farlow, 2013).

A promising alternative is the Multi-parent Advanced Generation Intercross (MAGIC) population, which offers a balanced alternative to biparental RILs and GWAS. MAGIC lines are developed by crossing multiple parents (normally 4-16) for several generations through structured mating designs, resulting in multi-parent RILs. The resulting lines have diverse genomic combinations of all founder lines and a higher recombination frequency (Figure 2) (Cavanagh et al., 2008; Kover et al., 2009; Mackay et al., 2014; Stadlmeier et al., 2018). Recombination events break up large blocks of linked genes and increase mapping resolution. This allows for narrowing down QTL regions more precisely than what might be possible in a biparental population (Cavanagh et al., 2008; Kover et al., 2009).

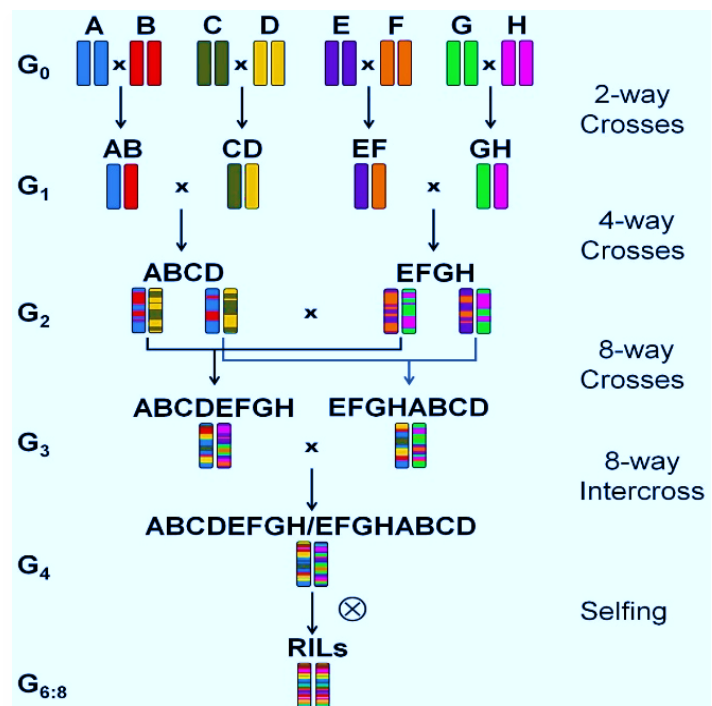


Figure 2. MAGIC RIL development. An 8-way cross in which 8 founders were inter-crossed for several generations, resulting in RILs with mosaics of parental genomes

In 2009, Kover et al. developed the first MAGIC population in *A. thaliana*, using 19 founder genotypes. The founders were chosen based on their broad geographical distribution or frequent use in genetic research. The Arabidopsis MAGIC population has recently been used to map traits such as natural variation in leaf zinc concentration, variation in root number and structure, and bolting time (Kover et al., 2009; López-Ruiz et al., 2024; Ricachenevsky et al., 2025). However, gas exchange-related traits, such as stomatal responses to elevated CO₂, have not yet been mapped using this population.

2 Aim and research objective

The main aim of this study was to identify QTL associated with the short-term stomatal response to elevated CO₂.

Additionally, QTL related to other gas exchange traits, including stomatal conductance at ambient (420 ppm) and elevated (800 ppm) CO₂ (Gs_420 and Gs_800 respectively), net photosynthesis at both CO₂ levels (P_420 and P_800), magnitude of stomatal conductance response to elevated CO₂, and half response time (half-time) were also mapped. To achieve this, the stomatal response was measured in a subset of 206 randomly selected recombinant inbred lines (RILs) from the MAGIC population of *A. thaliana* under controlled ambient and elevated CO₂ conditions. Specifically, the percentage reduction in stomatal conductance (% reduction in g_s) following CO₂ elevation was calculated and used as the primary trait for short-term stomatal response QTL mapping.

The half-response time, defined as the time taken for g_s to reach 50% of its total response after CO₂ elevation, was calculated and evaluated alongside the magnitude of response. All trait data were then used for QTL mapping to identify genomic regions associated with the observed phenotypic variation and were followed by candidate gene analysis in the identified *loci*.

3 Materials and methods

3.1 Plant materials and growth conditions

This study utilised the MAGIC RILs of *A. thaliana*, developed through crossing 19 founder accessions as explained by Kover et al., 2009. Seeds were obtained from the European Arabidopsis Stock Centre (NASC, <https://arabidopsis.info/>). A total of 206 RILs were randomly selected from a subset of 527 MAGIC lines using a random number generator (<https://www.random.org/>) to study the short-term response of stomatal conductance. - that is, the immediate change in stomatal opening within minutes to hours—under elevated CO₂ (800 ppm). Additionally, the 15 parental accessions, which were the only ones available from the NASC centre, were included in the experiment for comparison.

The MAGIC lines and their parental accessions were previously genotyped using 1,260 single-nucleotide polymorphism (SNP) markers, evenly distributed across the five chromosomes with an average spacing of approximately 96 kb, as described by Kover et al. (2009). The genotypic data are publicly available at <http://gscan.well.ox.ac.uk/arabidopsis>.

Seeds were sown in a peat–perlite mix (S-jord, Hasselfors garden) and cold-stratified at 4°C for two days to ensure uniform germination. After two weeks of initial growth, individual plants were transplanted into pots compatible with the Li-COR 6400XT gas exchange Arabidopsis chamber (Figure 3b). Three biological replicates were maintained for each RIL. Plants were grown in batches of 17–25 lines, with Arabidopsis Columbia-0 (Col-0) included in each batch as a control to ensure comparability between batches.

Plants were grown under controlled conditions in a climate chamber under the following conditions: 21°C day/18 °C night and 8/16 light/dark photoperiod, 70% relative humidity, and photosynthetically active radiation (PAR) of 150-200 $\mu\text{mol photons m}^{-2}\text{s}^{-1}$. The three replicates of each line were distributed randomly across two trays (Figure 3d). The trays were rotated 180° and moved clockwise on the shelf every two days to account for within-chamber variation.

3.2 Gas exchange measurements

Leaf gas exchange was measured in four-week-old *A. thaliana* rosettes (Figure 3a) using an LI-6400XT portable photosynthesis system (LI-COR Biosciences, USA) connected with an Arabidopsis chamber (6400-17A) with an RGB (red, green, blue) light source (Figure 4), following the methodology of Johansson et al. (2020). After 4 weeks of growth, a healthy plant was selected for each of the 206 RILs, ensuring that it was neither too small nor too large, with a rosette size fitting within the circumference of the pot. A single replicate per line was used for measurement. The whole-plant chamber is designed to conduct whole-rosette gas exchange measurements and can accommodate plants up to 7 cm in diameter and 1.5 cm in height. Measurements were conducted at an air temperature of 21°C, under a light intensity of 200 $\mu\text{mol photons m}^{-2}\text{s}^{-1}$, matching growth conditions. The airflow rate was set to 400 $\mu\text{mol s}^{-1}$ and the chamber fan to maximum speed. At the beginning of each measurement, once the plant was placed in the Arabidopsis chamber, an initial vapour pressure deficit (VPD) of approximately 1 ± 0.2 kPa is set as the target. This VPD is then maintained throughout the measurement process, with only minor variations of about ± 0.03 kPa. The soil surface was covered with cling film to ensure that moisture loss was primarily from the plant itself, and to prevent additional water vapour flux from the soil, which could otherwise affect the accuracy of transpiration measurements (Figure 3c).

In this measurement setup, leaf temperature is estimated indirectly using an energy balance equation, as it cannot be measured directly. This equation considers the variables such as light intensity and boundary layer conductance, the resistance to gas flow caused by still air around the leaf. Since boundary layer conductance could not be measured directly, a standard value of 4 mol $\text{H}_2\text{O m}^{-2}\text{s}^{-1}$ was used based on previous studies (Johansson et al., 2020). The Li-Cor system automatically performs this estimation when using the "energy balance" measurement mode, called whole plant chamber RGB_EB (where EB stands for energy balance). The stomatal ratio (ratio of number of stomata on the upper and lower leaf surfaces) was also set at 0.5, as recommended when precise values are unknown (LI-COR Biosciences, 2011).



Figure 3. (a) Individual MAGIC lines were transplanted into pots compatible with the LI-6400XT whole plant *Arabidopsis* chamber. (b) Three replicates per line were randomly distributed across two trays. Trays were rotated 180° and moved clockwise on the shelf every two days to reduce positional effects and variation within the growth chamber. (c) Four-week-old *Arabidopsis* rosettes. (d) Soil surface covered with cling film prevents soil evaporation.

Each plant was first measured at ambient CO₂ (420 ppm) level, and g_s was recorded after steady-state conditions were reached, which was defined as a change in g_s of less than 2.5% over five minutes. Once stable, three consecutive readings were taken at 10-second intervals. The CO₂ concentration was then elevated to 800 ppm, and the same procedure was followed to measure g_s at 800 ppm CO₂.

Gas exchange data are expressed per unit leaf area, meaning that measured values need to be normalised to the leaf area of the rosette. To determine the leaf area, the total of each plant was carefully excised after measurements were taken, and leaf images were captured using a flatbed scanner (Epson, Version: Perfection 3490 photo). The total leaf area of each plant was measured using the ROI Manager function in ImageJ software (version 1.54 g; Schneider et al., 2012).

The stomatal responses were analysed by calculating the percentage reduction in stomatal conductance (g_s) following CO₂ elevation from 420 ppm to 800 ppm CO₂. The percentage reduction was used to quantify the plant's short-term stomatal response, which was used as the primary trait for QTL mapping. This method helps to normalise the data across genotypes with varying baseline g_s values, allowing for a fair comparison of how each plant responds to elevated CO₂, regardless of initial stomatal conductance differences. By focusing on the relative change, the proportional change in stomatal conductance relative to the initial value was measured, rather than comparing absolute g_s values. In addition, other gas exchange variables were

extracted from the measurement data: g_s at 420 ppm and 800 ppm CO₂, net photosynthesis at both CO₂ levels, the magnitude of the response (absolute g_s response) that is the total decrease in stomatal conductance, calculated as the difference between g_s at 420 ppm and g_s at 800 ppm CO₂. The half-response time, the time taken to reach half of the magnitude response after CO₂ elevation, was also calculated. The half-response time provided insight into how quickly each genotype reacted to elevated CO₂, excluding the slower stabilisation phase that occurred at the end of the measurement. If the entire reaction time were considered, it would include the prolonged stabilisation phase, which is not relevant for assessing the time taken for stomatal response. This approach helped to analyse how quickly and how strongly each plant reacted to increased CO₂ in a way that made fair comparisons possible.



Figure 4. Gas exchange measurement setup using the LI-6400XT system fitted with a Whole plant *Arabidopsis* chamber (6400-17/A) and a red, green, blue (RGB) light source. The system was used to conduct gas exchange measurements in four-week-old *A. thaliana* rosettes under controlled conditions.

3.3 Trait distribution and regression analysis

Regressions were performed using JMP version 18 Student Edition (SAS Institute, USA). To assess data distribution, histograms were created for each trait: % reduction in g_s , stomatal conductance at 420 ppm and 800 ppm CO₂ (G_s_{420} , G_s_{800}), net photosynthesis at 420 ppm and 800 ppm CO₂ (P_{420} and P_{800}), leaf area, half-response time, and magnitude responses. Among these, G_s_{420} , G_s_{800} , P_{420} , and leaf area showed a right-skewed distribution. These traits were log-transformed to improve normality before analysis. Additionally, scatter plots fitted with linear regression models were used to examine potential relationships between physiological traits such as G_s_{420} vs P_{420} , G_s_{420} vs half-time, % reduction in g_s vs half-time and magnitude response vs half-time.

3.4 QTL mapping

QTL mapping and the following analyses, including SNP association scan and QTL support interval analysis, were performed using R software (version 4.4.2). The R/qtl2 package (Broman, 2019) was used for the analyses, and data visualisation was performed using ggplot2 (Wickham, 2016). R/qtl2 is designed to accommodate complex genotypes, such as those found in MAGIC populations. QTL mapping was carried out for all traits measured in this study, including % reduction in g_s , G_s_{420} , G_s_{800} , P_{420} and P_{800} , leaf area, half-response time, and magnitude responses to identify genomic regions associated with these traits.

The package included an example dataset for 19-way MAGIC QTL mapping. Genotypic and phenotypic data files for this study were prepared using these example files as a template. The example files were already formatted to meet the requirements of R/qtl2. The genotype file for the current study was prepared by filtering to include only the MAGIC lines used in this study, and the phenotype file was updated with the measured traits.

A genome-wide scan for QTLs was conducted using Haley-Knott regression (Haley and Knott, 1992), a computationally efficient method for detecting associations between genetic markers and phenotypic traits. This method provides a fast approximation of standard interval mapping, which is a common approach in many QTL mapping studies (Lander et al., 1989). A major advantage of this method is that, in addition to testing the association between genetic markers and the trait of interest, it also examines the regions between the markers. Genotypes between markers are statistically inferred based on the genotypes of surrounding markers and the recombination frequency. This allows the method to scan between real markers as well, making it possible to estimate the location of a QTL more precisely, even if it is not located directly on a known marker (Lander et al., 1989; Xu, 2013). A basic QTL mapping method uses single-QTL models that test one phenotypic trait at a time for associations with genetic markers. Advanced models can analyse multiple traits simultaneously and detect interactions between QTLs across traits. However, due to the complexity of MAGIC RIL populations, the R package currently used for this analysis, R/qtl2, supports only single-QTL models and does not allow for multi-trait analysis or detection of epistatic interactions. Therefore, each trait must be analysed separately (Broman et al., 2019).

To measure the strength of the association between genetic markers and a trait across the genome, the Logarithm of Odds (LOD) score is calculated at each position in the genome. Higher LOD scores indicate stronger evidence for a QTL at that position. To determine whether the observed LOD scores are statistically significant, a permutation test with 1,000 permutations of the phenotypic data was done while keeping the genotypic data intact. This test helps to generate a threshold value for the LOD score (Churchill and Doerge, 1994; Broman et al., 2019). Significant QTL peaks were identified by comparing observed LOD scores against permutation-derived thresholds. The peak exceeding the significance threshold was further analysed to identify the genomic regions associated with the trait of interest.

The position of QTL obtained through this analysis carries some uncertainty. Therefore, it is important to define a support interval around the peak position to indicate the range within which the true genomic region may be present. Two methods were used to narrow down the QTL region: the 1.5-LOD support interval and the Bayesian Credible Interval (BCI). The 1.5-LOD support interval defines the region around the peak of the LOD score where the value

remains within 1.5 units of the highest LOD score. This range represents the most likely location of the QTL, with flanking markers that are genetically linked to the trait (Broman & Sen, 2009).

The BCI provides an alternative way to estimate the possible location of a QTL, which uses Bayesian principles to generate a probability distribution for where the QTL might be located. While both methods are commonly used, BCI has been shown to be more consistent (Broman & Sen, 2009).

3.5 Candidate gene analysis

To identify potential candidate genes within the region of the QTL associated with percentage g_s reduction in response to elevated CO_2 , two approaches were employed:

First, a SNP association scan was conducted throughout the genome using a R/qtl2 function to detect SNP markers strongly associated with the trait. Within the QTL interval of % reduction in g_s trait, SNPs were ranked based on their LOD scores, where higher scores indicate a stronger association with the trait. This helped prioritise markers most likely linked to genetic variation affecting g_s responses. Secondly, all annotated loci within the BCI interval (21.94–29.89 Mbp on chromosome 1) were retrieved from The Arabidopsis Information Resource (TAIR) database (<https://www.arabidopsis.org>). The initial list was filtered to include only protein-coding genes. Genes were evaluated based on known functions, involvement in stomatal regulation, CO_2 signalling, ABA pathways, or general stress responses. To further prioritise candidates, functional annotations and published mutant phenotype data were reviewed. To assess the relevance of the shortlisted genes to stomatal function, their expression in guard cells was also examined using TAIR.

3.6 Data cleaning and transformation

After obtaining the initial mapping results, data were re-assessed for potential outliers. During this process, two outliers were identified. Based on a careful review of the sample history and measurement methods, these outliers were removed to improve data reliability. Following this, the distributions of all traits were again analysed using histograms. All the traits except for “% reduction in g_s ” showed a right-skewed distribution; they were therefore log-transformed to improve normality. The transformed dataset was then used for a second round of QTL mapping.

4 Result

4.1 Descriptive statistics of gas exchange traits

Gas exchange parameters were recorded from four-week-old *Arabidopsis* rosettes using an LI-6400XT portable photosynthesis system fitted with an *Arabidopsis* whole-plant chamber and a RGB light source. Short-term responses to elevated CO₂ were measured continuously, beginning at ambient CO₂ level (420 ppm) and transitioning to elevated CO₂ level (800 ppm) for both parent lines and the MAGIC lines. The g_s was recorded after steady-state conditions were achieved at both CO₂ levels, showing an overall reduction in g_s across all RILs (Figure 5) and parents.

At ambient CO₂ (420 ppm), the g_s across the 206 MAGIC lines ranged from 0.08 to 0.43 mol H₂O m⁻² s⁻¹, while at elevated CO₂ (800 ppm), values ranged from 0.05–0.24 mol H₂O m⁻² s⁻¹. The percentage reduction in g_s following CO₂ elevation varied between 7% and 54%, with a mean reduction of 29%. The magnitude of g_s response ranged from 0.006–0.19 mol H₂O m⁻² s⁻¹, while the half-response time (time until half the magnitude of the response was achieved) ranged from 7 to 16 minutes. Photosynthesis rates at ambient and elevated CO₂ also varied, spanning 4.32 to 11.33 μmol CO₂ m⁻² s⁻¹ and 5.56–15.22 μmol CO₂ m⁻² s⁻¹, respectively.

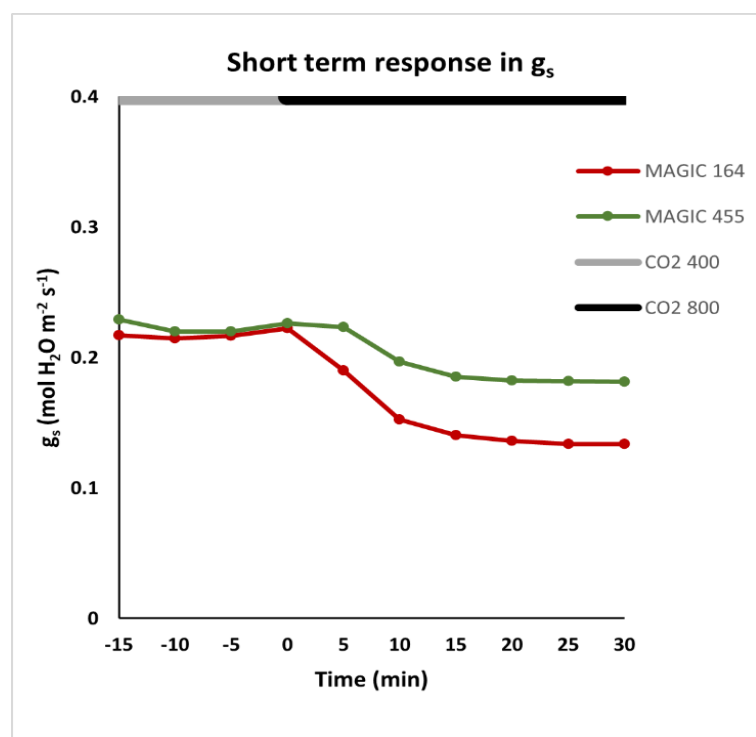


Figure 5. A decline in stomatal conductance (g_s) was observed in MAGIC RILs when exposed to short-term elevation of CO₂ from ambient levels (420 ppm) to 800 ppm during gas exchange measurements.

Data distribution for all traits was analysed using histograms (Figure 6), including stomatal conductance at 420 ppm (Gs_420) and 800 ppm (Gs_800) of CO₂, % reduction in g_s, half-response time, magnitude response and net photosynthesis at 420 ppm (P_420) and 800 ppm (P_800). These histograms illustrate the frequency distributions of trait values observed across 206 plant samples. % reduction in g_s showed a near normal distribution and was therefore not transformed throughout the analysis (Figure 6). The traits Gs_420, Gs_800, P_420, P_800, half-time, and magnitude response displayed a right-skewed distribution. To improve normality before QTL analysis, these six variables were log-transformed (Figure 7).

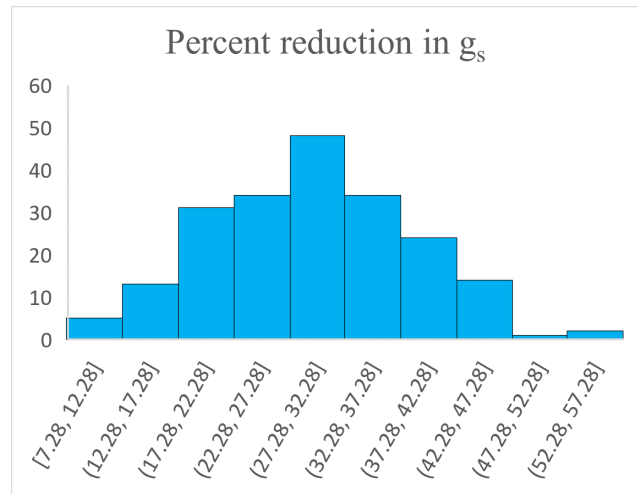


Figure 6. The data obtained for the variable “percent reduction in stomatal conductance (g_s)” (%) in MAGIC lines (n= 206) under elevated CO₂ follows a near normal distribution.

Gas exchange measurements were also conducted with 15 parental lines to assess variability among the parents. The parental lines showed considerable variation across all measured traits (Table 1). % reduction in g_s ranged from 19.80% to 36.86%. Gs_420 values ranged from 0.11 to 0.20 mol H₂O m⁻²s⁻¹, and Gs_800 from 0.07 to 0.14 mol H₂O m⁻²s⁻¹. P_420 ranged from 5.64 to 7.14 μmol CO₂ m⁻²s⁻¹, and P_800 from 7.60 to 9.36 μmol CO₂ m⁻²s⁻¹. Half-time ranged from 4.14 to 10.02 minutes. These values demonstrate significant variability in trait performance among the parental lines. Stomatal conductance was also measured in the control line Col-0, one of the parent lines. It was grown alongside each batch to ensure comparability.

Table 1. The 15 parent lines exhibit differences in trait values across the various traits assessed, reflecting the diversity in performance among the lines.

Percent reduction in g _s (%)	Gs_420 (molH ₂ O m ⁻² s ⁻¹)	Gs_800 (molH ₂ O m ⁻² s ⁻¹)	P_420 (μmolCO ₂ m ⁻² s ⁻¹)	P_800 (μmolCO ₂ m ⁻² s ⁻¹)	¹ Half-response time (minute)
19.80 – 36.86	0.11- 0.20	0.07- 0.14	5.64-7.14	7.60-9.36	4.14-10.02

¹time until half the magnitude of the response was achieved (minutes)

Col-0 from different batches showed a consistent response of g_s to elevated CO_2 (ranging from 31.6% to 36.5%).

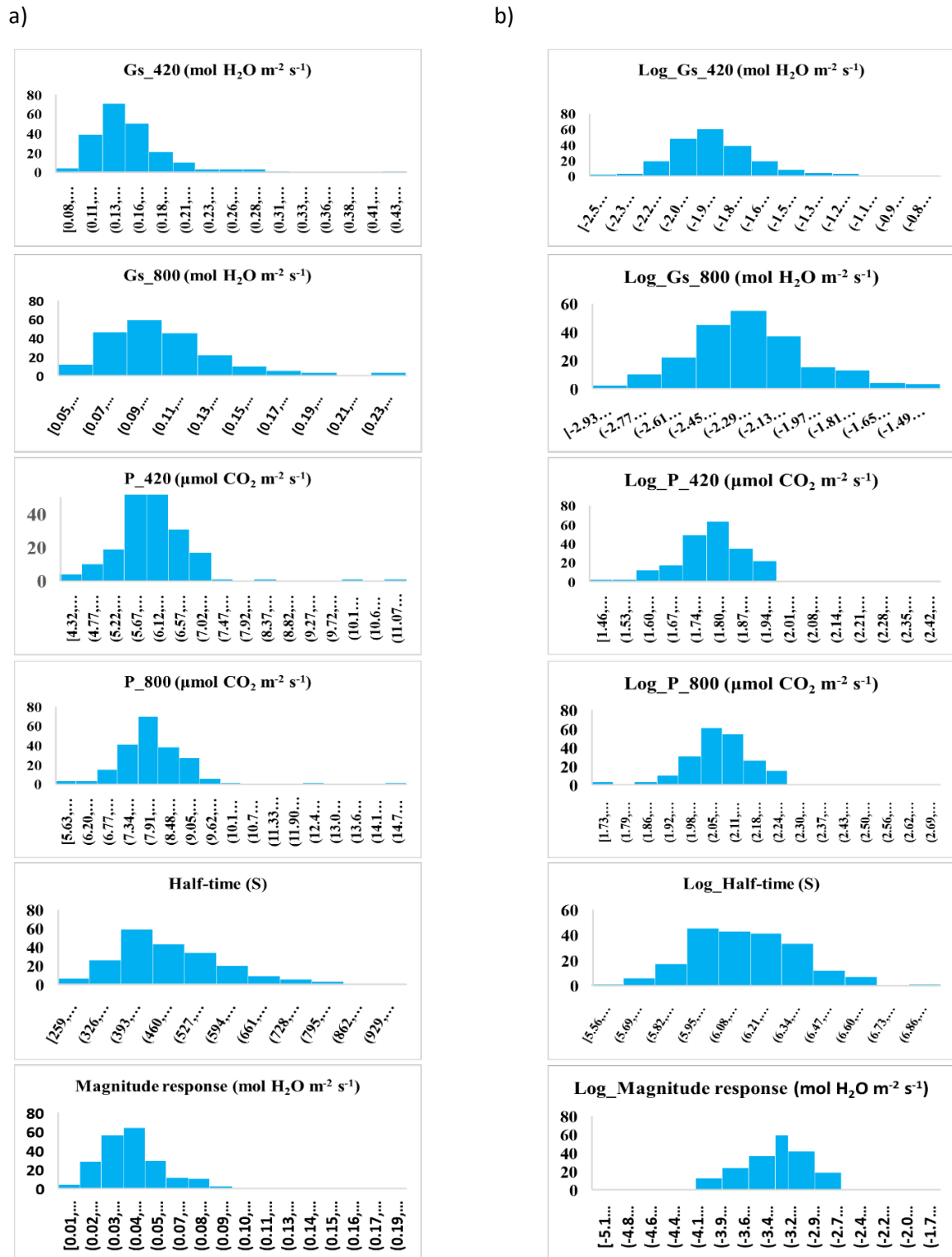


Figure 7. a) The original data distribution for the traits: stomatal conductance at 420 and 800 ppm CO_2 (Gs_{420} and Gs_{800}), photosynthesis at 420 and 800 ppm CO_2 (P_{420} and P_{800}), leaf area, half-time (the time required to reach half of the total stomatal response after CO_2 elevation), and magnitude of response (the total stomatal response to elevated CO_2 at 800 ppm), measured for 206 samples ($n = 206$). Panel b shows the distribution of the same traits after log-transformation

4.2 Correlation of different gas exchange traits

Relationships between key physiological traits were analysed using scatter plots. First, the relative response in g_s (% reduction) was compared with the time taken to reach half of the g_s response to increased CO_2 (Figure 8). This was done to check if the size of the response has any link with how fast the response happens. However, no clear relationship was found. One possible reason is that if the starting g_s is very low, a small change in g_s can look like a big response when expressed as a percentage change. Next, the actual magnitude of the g_s response (the difference between g_s at 420 ppm and 800 ppm) was compared with the half-response time (Figure 9). This also did not show any correlation.

Lastly, the relationship between the g_s and P_{420} at 420 ppm CO_2 ($G_{s_{420}}$ and P_{420}) was tested using linear regression. The result showed a significant relationship ($F_{1,204} = 28.6$; $P < 0.0001$; $R^2 = 0.12$) (Figure 10). However, the low R^2 means that only 12% of the variation in photosynthesis is explained by g_s . This result suggests that g_s and photosynthesis are co-regulated to some extent, but a large part of the variation in photosynthesis is not caused by stomatal conductance.

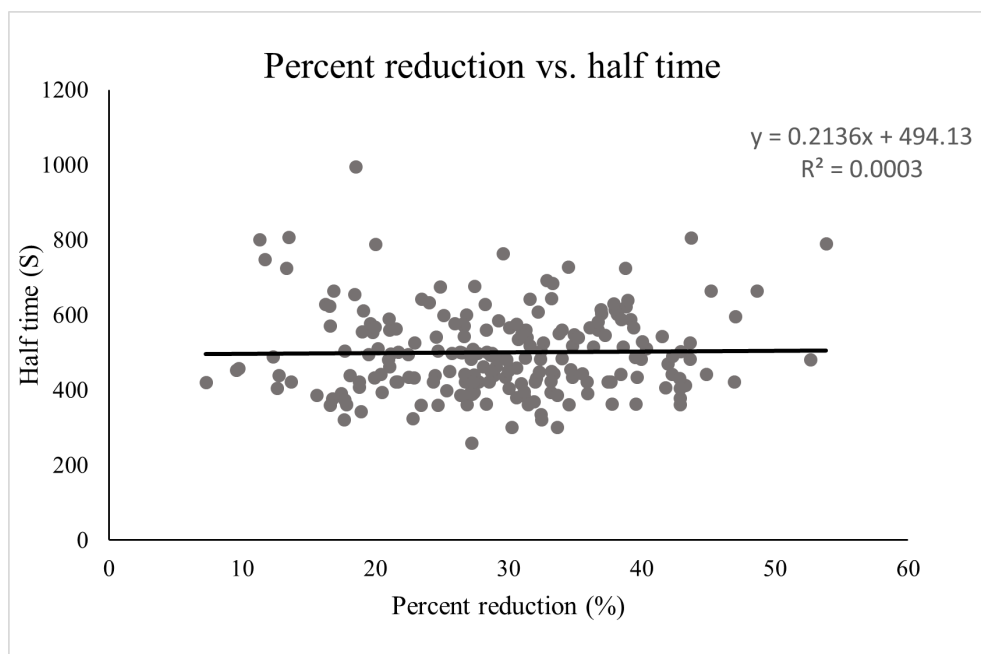


Figure 8. Relationship between the percentage reduction in stomatal conductance (%) at elevated CO_2 and the half-time (s) required to achieve 50% of the g_s response following CO_2 elevation from 420 ppm to 800 ppm among MAGIC lines. Each point represents an individual plant measurement ($n = 206$). The data show no significant correlation between the percentage of stomatal conductance reduction and the response timing.

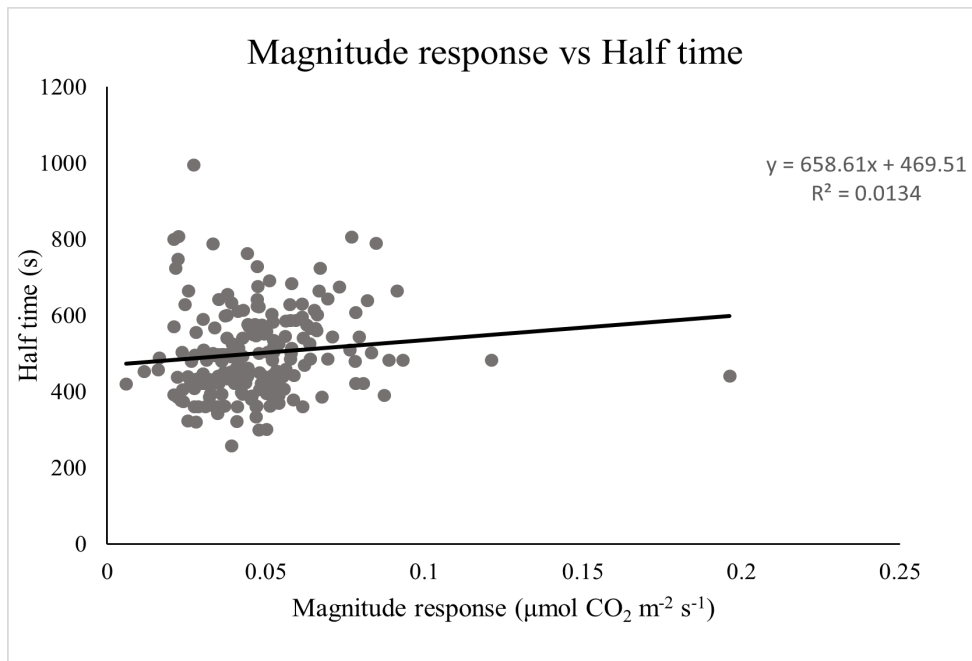


Figure 9. Relationship between the magnitude of stomatal conductance (g_s) reduction following CO_2 elevation and the half-time(s) required to reach 50% of the total g_s response among MAGIC lines. Each point represents an individual plant measurement ($n=206$). The magnitude of the response reflects the extent of stomatal closure when CO_2 concentration increased from ambient (420 ppm) to elevated levels (800 ppm). The data show no significant correlation between the degree of stomatal conductance reduction and the speed of the response.

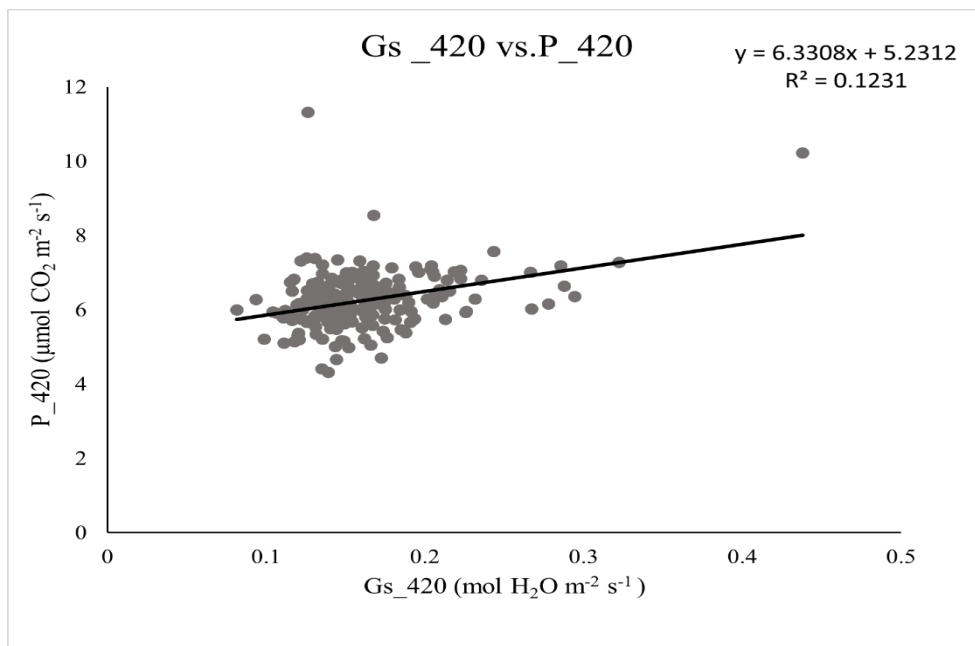


Figure 10. Relationship between stomatal conductance (G_{420} units: $\text{mol H}_2\text{O m}^{-2} \text{s}^{-1}$) at ambient CO_2 (420 ppm) and photosynthesis rate (P_{420} ; units: $\mu\text{mol CO}_2 \text{m}^{-2} \text{s}^{-1}$) at 420 ppm CO_2 among MAGIC lines. Each point represents an individual plant measurement ($n = 206$).

4.3 QTL mapping for gas exchange traits

Genome-wide QTL scans were performed with Haley-Knott regression separately for all seven traits using the R/qt12 package (Broman et al., 2019). Significance of QTLs was determined using LOD thresholds derived from 1,000 permutations at $\alpha = 0.05$.

In the first round of analysis, using the original data (without removal of outliers), a significant QTL was identified for the trait % reduction in g_s on chromosome 1 at 26.40 Mega-base pairs (Mbp) (Table 3). The threshold cut-off was LOD = 10.2, and the maximum LOD was 10.3, meaning the QTL peak exceeded the threshold (Figure 11). All the other traits were analysed with their respective LOD plots and thresholds to check for any potential QTLs. No other traits showed significant QTLs, although minor peaks were observed (Figure 12). A summary of threshold values for all traits is provided in Table 2.

A second round of QTL mapping was conducted using a cleaned version of dataset. During this step, two outliers were identified and removed after a thorough review. Following removal of these outliers and reassessment of the distribution of data for all traits, the data for half-response time was found to require log transformation to improve normality. Using this updated dataset, a significant QTL was detected for half-response time (maximum LOD = 10.6, significant LOD = 10.4), one that had not been identified in the original analysis (Figure 11). The QTL detected is located at the end of chromosome 1 at 29.32 Mbp (Table 3).

Additionally, the magnitude of the response also showed a peak just below the significance threshold (peak LOD = 10.6, LOD threshold = 10.9), on the same chromosome at 23.88 Mbp. The QTLs for the magnitude and speed of the response share their support intervals with the QTL for the % reduction in g_s . Notably, the QTL for % reduction in g_s remained consistent before and after removal of outliers. As the additional significant QTL (for half-response time) was detected at a later stage in the project, candidate genes in the region that did not overlap with the QTL for percent reduction could not be investigated within the scope of this project.

Table 2. Significant thresholds for each phenotypic trait in MAGIC lines, determined through 1000 permutations. Any QTL peak with a LOD score above this cut-off value is considered significant

Percent reduction in g_s	¹ Gs_420	² Gs_800	³ P_420	⁴ P_800	⁵ Half-response time	⁶ Magnitude response
10.2	11	10.6	11.1	11.6	10.4	10.9

¹Stomatal conductance at 420 ppm CO₂, ²Stomatal conductance at 800 ppm CO₂, ³Net photosynthesis at 420 ppm CO₂, ⁴Net photosynthesis at 800 ppm CO₂, ⁵time required for the stomata to give half of the total response when CO₂ is elevated from 420 ppm to 800 ppm, ⁶the total amount of response shown by stomata when CO₂ is elevated from 420 ppm to 800 ppm

Table 3. Two significant QTLs detected on chromosome 1 in MAGIC lines for two physiological traits; the trait percent reduction in stomatal conductance (% reduction) at elevated CO₂ and the half-time (s) required to reach 50% of the g_s response after CO₂ was increased to 800 ppm

Variable	Chromosome	Position (Mbp)*	Maximum LOD	Significant LOD
Percent reduction	1	26.405130	10.3	10.2
Half-time	1	29.321880	10.6	10.4

*Mega-base pair

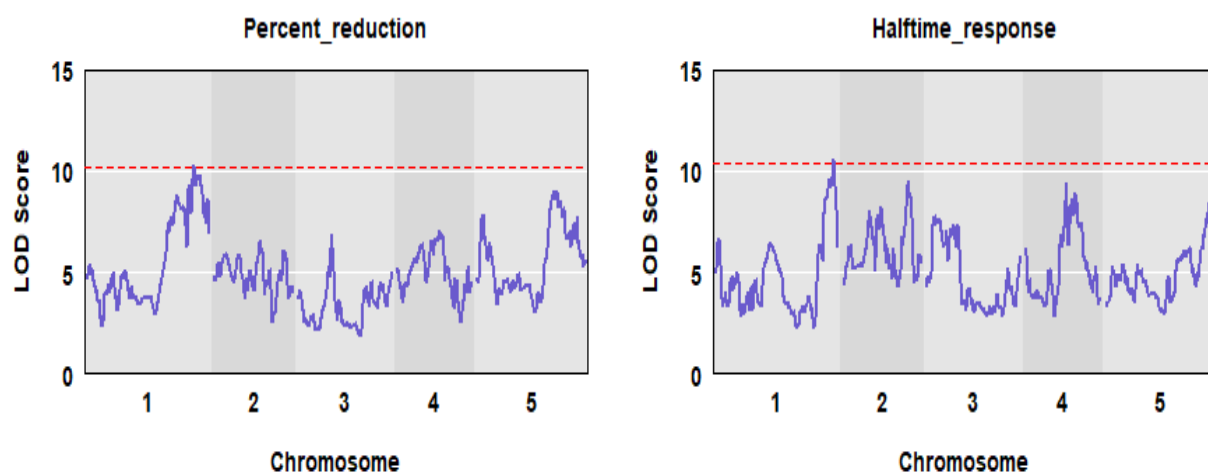


Figure 11. LOD score plots of physiological traits percent reduction and half-time in MAGIC lines using Haley-Knott regression with the R/qtl2 package. A significant QTL was identified for the traits percent reduction in stomatal conductance (g_s) (%) at elevated CO₂ and the half-time (s) required to achieve 50% of the g_s response following CO₂ elevation to 800 ppm at the end of chromosome 1 (position: 26.41 mega-base pair and 29.32 mega-base pair, respectively). The horizontal red dashed line represents the cut-off (significant LOD), with LOD = 10.2 and 10.4, and the maximum LOD scores of 10.3 and 10.6 for both traits, respectively.

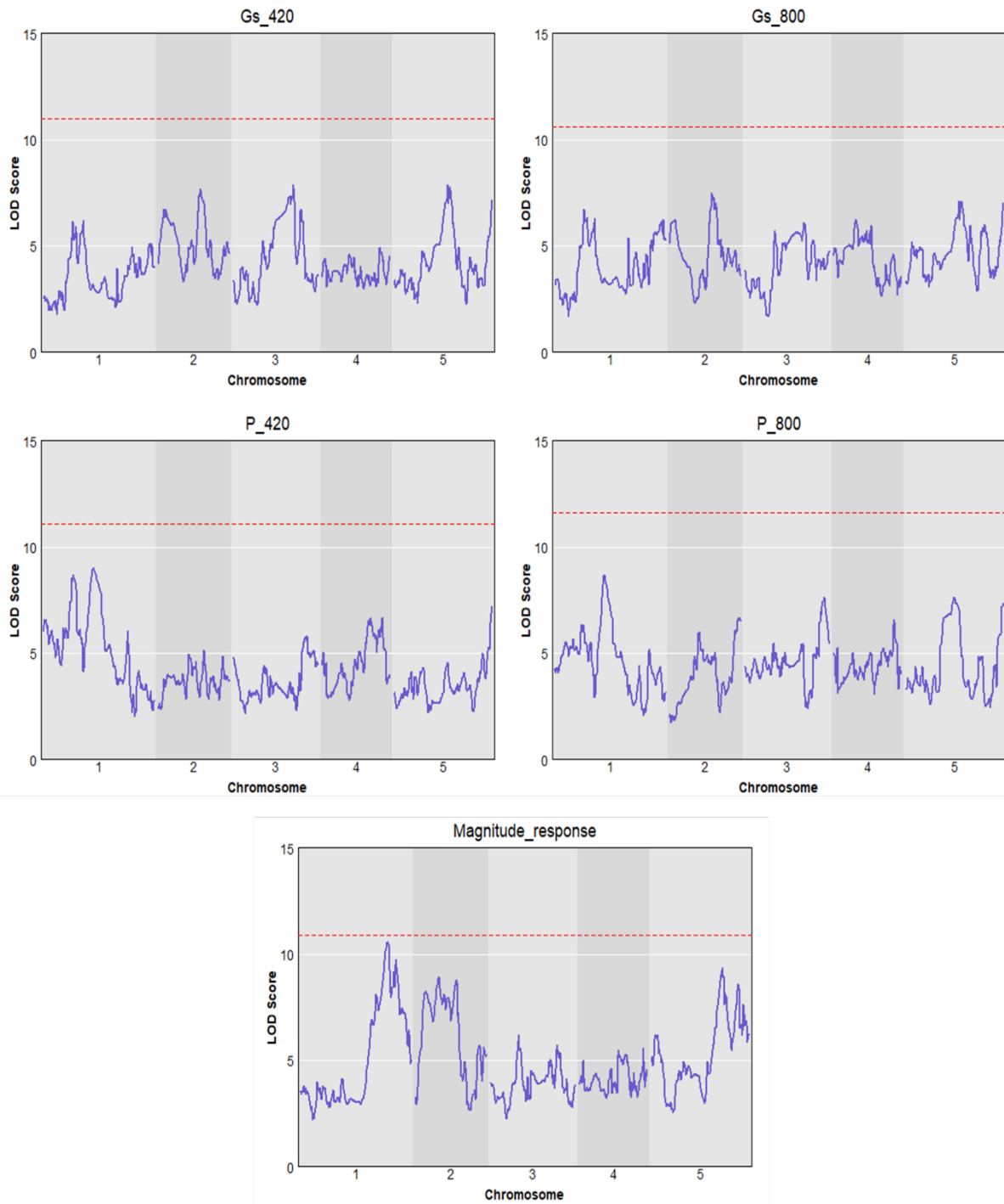


Figure 12. Genome-wide QTL scans for six physiological traits in MAGIC lines using Haley-Knott regression with the R/qtl2 package. LOD score plots are shown for the following traits: stomatal conductance at 420 ppm CO₂ (Gs_420), stomatal conductance at 800 ppm CO₂ (Gs_800), photosynthesis at 420 ppm CO₂ (P_420) and 800 ppm CO₂ (P_800) and magnitude response, the amount of stomatal conductance reduction following CO₂ elevation from 420 ppm to 800 ppm. Each subplot includes a horizontal reference line indicating the trait-specific permutation-derived LOD significance threshold ($\alpha = 0.05$). No significant QTLs were detected for these traits. However, a notable peak was observed for magnitude response near the end of chromosome 1. The respective significance thresholds were: Gs 420: LOD = 11, Gs 800: LOD = 10.6, P_420: LOD = 11.1, P_800: LOD = 11.6, Magnitude response: LOD = 10.9.

4.4 QTL support interval

To assess the range of the QTLs detected for % reduction in g_s and half-response time, both the 1.5-LOD support interval and the Bayesian credible interval (BCI) were used. The 1.5-LOD interval for the percent reduction significant QTL ranged from 22.29 Mbp to 28.83 Mbp, while the BCI spanned from 22.35 Mbp to 28.66 Mbp, with the QTL peak located at 26.41 Mbp (Figure 13). For half-response time, the 1.5-LOD interval ranged from 27.65 Mbp to 29.81 Mbp, and the BCI ranged from 27.85 Mbp to 29.69 Mbp, with the peak positioned at 29.32 Mbp (Figure 14). These intervals help narrow down the regions for identifying flanking markers.

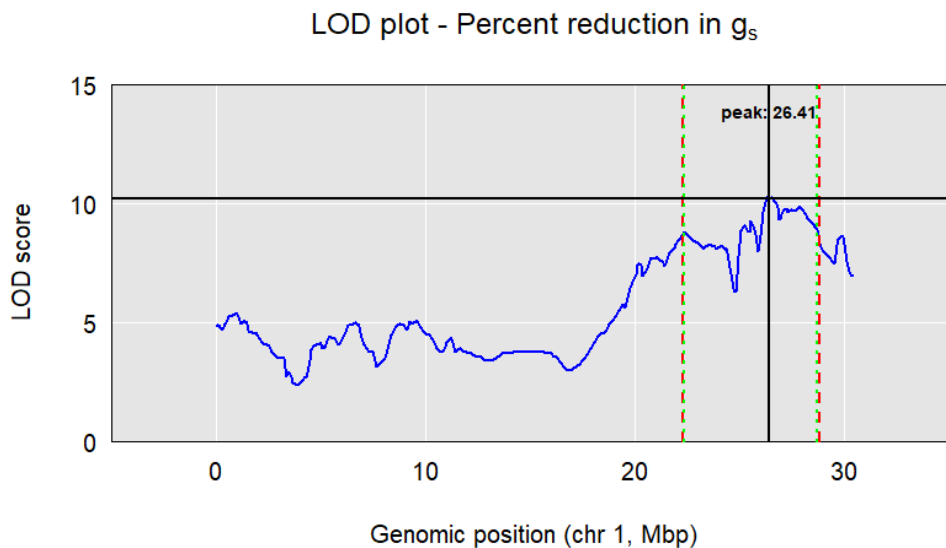


Figure 13. The 1.5-LOD support interval (the range where the LOD score is within 1.5 units of the maximum) and the Bayesian Credible Interval (BCI) (to give the range of QTL peak in the genome area) of a detected QTL for percent reduction in stomatal conductance (g_s) at elevated CO_2 (800 ppm) on chromosome 1. The blue line represents the LOD score across all genomic positions with a maximum LOD of 10.3. The 1.5-LOD support interval (red dotted lines) defines the most likely QTL region (22.35 Mbp (Mega-base pair) to 28.66 Mbp) for 1.5 support interval, while the BCI (green dotted lines) spanned from 22.28 to 28.83 Mbp. A significance threshold of $LOD = 10.2$ (black horizontal line) is applied to assess statistical relevance. The peak LOD score is observed at 26.41 Mbp (black vertical line), marking this position as the most probable QTL location.

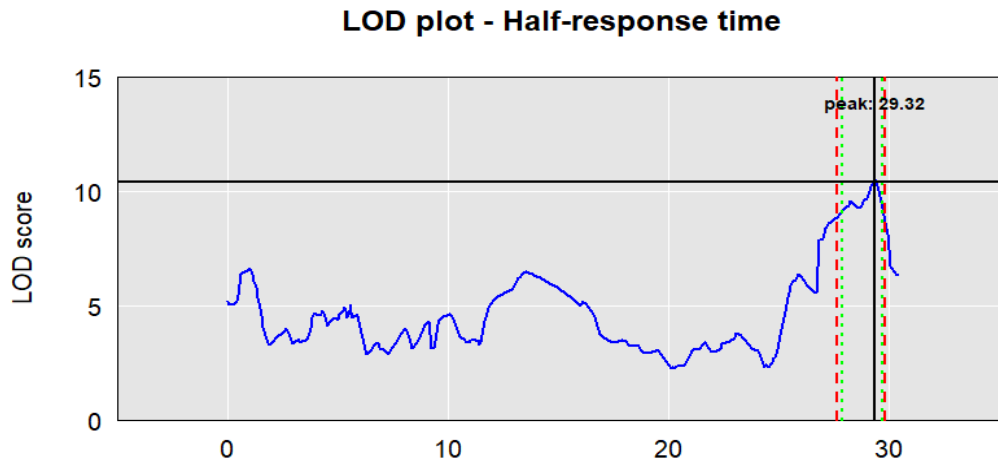


Figure 14. The 1.5-LOD support interval (the range where the LOD score is within 1.5 units of the maximum) and the Bayesian Credible Interval (BCI) (to give the range of QTL peak in the genome area) of a detected QTL for half-response time (time for stomata to show 50% of total reaction when exposed to elevated CO₂) on chromosome 1. The blue line represents the LOD score across all genomic positions with maximum LOD=10.6. The 1.5-LOD support interval (red dotted lines) defines the most likely QTL region (27.64 Mbp (Mega-base pair) to 29.81 Mbp) for 1.5 support interval, while the BCI (green dotted lines) spanned from 27.85 to 29.69 Mbp. A significance threshold of LOD = 10.4 (black horizontal line) is applied to assess statistical relevance. The peak LOD score is observed at 29.32 Mbp (black vertical line), marking this position as the most probable QTL location.

4.5 SNP association scan

To identify the SNP most strongly linked to the QTL for % reduction in g_s , a genome-wide SNP association scan was performed (Figure 15). From this, SNPs located within the BCI interval (22.35–28.66 Mbp) on chromosome 1 were prioritised based on their LOD scores. This was done to find which SNPs in the QTL region have the strongest association with the trait. Higher LOD scores mean stronger associations. The top five SNPs within this interval showing the highest LOD scores were shortlisted for further analysis (Table 4). Among them, the SNP marker MN1_26787727, located about 377 kb downstream of the QTL peak, showed the highest association (LOD = 3.28). Since this SNP is close to the peak at 26.41 Mbp and falls within both the 1.5-LOD support interval and the BCI range, it was considered a strong candidate.

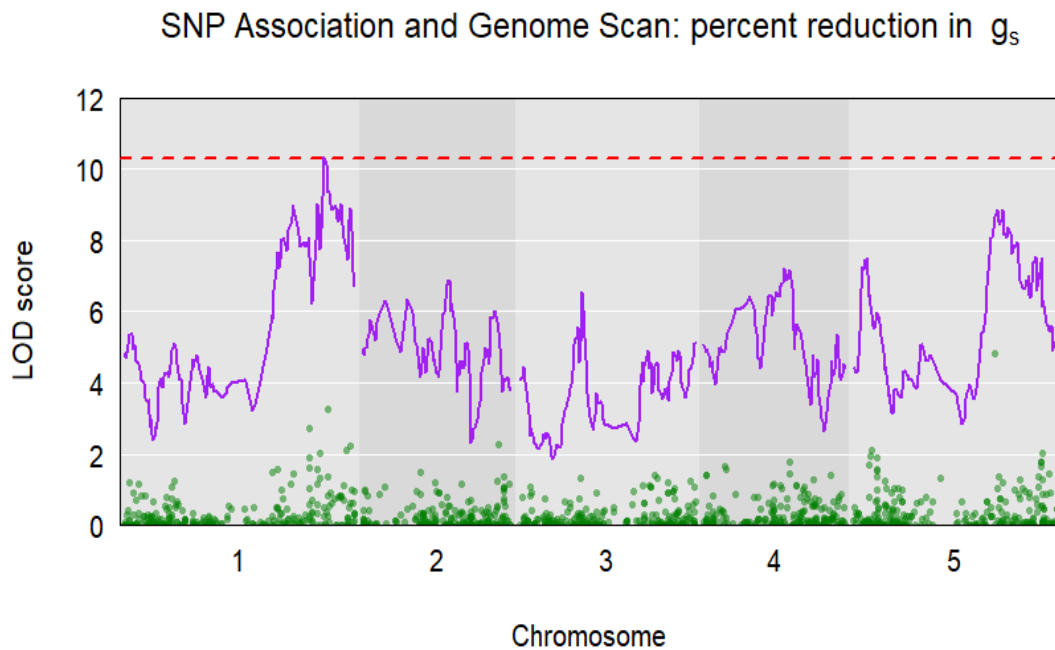


Figure 15. SNP association scan for the physiological trait percent reduction in stomatal conductance (g_s) in response to elevated CO_2 . The plot combines the genome-wide QTL scan for percent reduction in g_s , with SNP association results shown as green dots. The Y-axis represents LOD scores, and the X-axis denotes chromosomal positions across all five chromosomes. The red dashed line indicates the significance threshold for this trait (LOD = 10.2).

Table 4. Top five SNP markers associated with the QTL for percent reduction in g_s . These SNPs were identified based on their LOD scores from SNP association analysis within the 1.5-LOD support interval on chromosome 1. Genomic positions are given in mega base pairs (Mbp). The top SNP, MN1_26787727, had the highest LOD score (3.28) and was selected for further analysis of candidate genes

SNP Marker	LOD score	Physical position in chromosome (Mbp)
MN1_26787727	3.27	26.784065
FT_3485	2.71	24.333548
NMSNP1_29898175	2.21	29.893282
MN1_29326678	2.09	29.321713
PERL0235052	2.04	25.849927

4.6 Candidate Gene Analysis

Candidate genes for the QTL associated with % reduction in g_s were identified by combining results from the SNP association scan and functional gene annotations within the QTL support interval, retrieved from TAIR.

4.6.1 SNP-Associated Gene

The SNPs MN1_26787727, was considered the strongest candidate based on its high LOD score and close position to the QTL peak. This SNP falls within the gene called FAB1C (Formation of Aloid and Binucleate Cell 1C), which codes for a protein phosphatidylinositol-3-phosphate 5-kinase (PI3P5K) involved in the synthesis of phosphatidylinositol 3,5-bisphosphate (PtdIns(3,5)P₂).

In *A. thaliana*, loss-of-function mutants of PI3P5Ks, including FAB1C, showed delayed stomatal closure in response to abscisic acid (ABA), due to impaired vacuolar acidification and morphological changes in guard cells that are essential for rapid volume reduction during stomatal closure (Bak et al., 2013). Further studies revealed that PtdIns(3,5)P₂ does not directly stimulate vacuolar proton pumps; instead, it regulates ion channels such as Chloride Channel a (CLC-a) on the vacuolar membrane, critical for vacuolar acidification and the stomatal response (Carpaneto et al., 2017).

4.6.2 1.5-LOD Support Interval Linked Genes

The 1.5-LOD support interval region spanning from 21.94 Mbp to 29.89 Mbp contains approximately 2,000 protein-coding genes. To identify potential candidate genes, a keyword-based search was performed in the annotation information downloaded from TAIR. The search included keywords relevant to stress responses, stomatal regulation and signalling, such as stomata, stomatal conductance, guard cell, kinase, CO₂, carbonic anhydrase, plasma membrane, environmental stress, abiotic stress, stress responses, ABA signalling, and ion channel, recognizing that ABA and CO₂ signalling pathways converge downstream. This resulted in a list of 14 genes, in addition to the SNP-associated gene FAB1C, (Table 5).

The shortlisted genes (in bold) within the QTL interval fall into three broad functional categories based on their annotations and known or predicted involvement in stomatal regulation and stress signaling.

The first group includes three well-characterized genes directly linked to CO₂-induced stomatal closure. **βCA4** is located approximately 120 kb upstream of the identified QTL peak, plays a key role in catalysing the conversion of CO₂ into HCO₃⁻, a key early step in CO₂ signal transduction (Hu et al., 2010). In contrast, **βCA6**, although homologous, play only a minor role in this process. Last gene in this group is **HT1**, a kinase which works as a negative regulator of stomatal closure in response to elevated CO₂ (Töldsepp et al., 2018; Takahashi et al., 2022). HT1 lies about 3.31 Mb downstream of the QTL peak.

The second category includes six kinases that might be involved in stress signalling and stomatal regulation. a) **VPS34** (Vacuolar Protein Sorting 34), a phosphatidylinositol 3-kinase (PI3K) involved in dark-induced stomatal closure (Takahashi et al., 2017), b) **PI4P5Ks** (Phosphatidylinositol 4-Phosphate 5-Kinases), which helps in integrating environmental and

hormonal signals based on gene expression studies in *A. thaliana* (Lin et al., 2004). c) **SnRK2.10** (Snf1-Related Protein Kinase 2.10) belongs to the SnRK2 kinase family, which includes SnRK2.6 (OST1)—a key component of the abscisic acid (ABA)- and CO₂-induced stomatal closure pathway. However, the specific role of the candidate gene SnRK2.10 in this signalling context remains unclear (Wang et al., 2023). d) **MAPK15** (Mitogen-Activated Protein Kinase 15) is a member of the MAP kinase family, which is involved in plant signalling responses to various biotic and abiotic stimuli, including ABA. While MAPKs such as MAPK4 and MAPK12 are already known to play key roles in CO₂-induced stomatal closure, MAPK15 emerges as a candidate gene whose specific function in this pathway remains to be determined (Töldsepp et al., 2018). e) **SK42** (Shaggy-Like Kinase 42), which is also known as plant GSK3 (Glycogen synthase kinase), is involved in various stress responses (Song et al., 2023), and f) **MPK2** (Mitogen-Activated Protein Kinase 2), which responds to various abiotic stress signals (Ortiz-Masia et al., 2007).

The third group includes a variety of functionally diverse genes related to stress responses and stomatal behaviour. **JAC1** (J-Domain Protein Required for Chloroplast Accumulation Response 1), primarily functioning in chloroplast movement, also affects photosynthetic efficiency, stomatal aperture, water vapor conductance, and CO₂ uptake, in addition to takes part in photooxidative stress signaling (Czarnocka et al., 2020). **WDL7** (Wave-Dampened2-Like 7) encodes a protein that stabilises microtubules and is targeted for degradation during drought or ABA treatment by the E3 ubiquitin ligase MREL57 (Microtubule-Related E3 Ligase 57). This regulated degradation of WDL7 enables microtubule disassembly, facilitating stomatal closure (Dou et al., 2021). Another key gene is **JMJ17** (Jumonji Domain-Containing Protein 17), a histone demethylase involved in dehydration stress response by modulating the expression of OST1, a central kinase involved in ABA and CO₂ signalling (Huang et al., 2019). Lastly, SLAC1 HOMOLOGUE 1 (**SLAH1**) and SLAC1 HOMOLOGUE 4 (**SLAH4**) are anion channel proteins similar to SLAC1, which mediates ion efflux from guard cells to trigger stomatal closure in response to ABA and elevated CO₂ (Negi et al., 2008; Xue et al., 2011; Hōrak et al., 2016). Each gene was selected based on its function and what is known in the literature about its role in CO₂-induced stomatal movement.

Table 5. Candidate genes identified from SNP association scan and within the 1.5-LOD support interval (21.94–29.89 Mbp) on chromosome 1. These genes are linked to the QTL for % reduction in g_s and are prioritized based on their proximity to SNP markers within the identified region

Gene ID	Gene Name	Gene Function	Biological Relevance	References
SNP marker associated gene				
AT1G71010	FAB1C (Formation of Aploid and Binucleate Cell 1C)	Encodes a phosphatidylinositol-3p 5-kinase (PI3P5K), involved in synthesis of PtdIns(3,5)P ₂ .	Involved in vacuolar acidification and FAB1C mutants show delayed stomatal closure in response to ABA	Bak et al., 2013; Carpaneto et al., 2017

QTL peak 1.5 LOD interval associated genes

AT1G70410	β CA4 (Beta Carbonic Anhydrase 4)	Encodes the β -carbonic anhydrase 4 involved in CO ₂ sensing	Known upstream regulator in CO ₂ -induced stomatal closure	Hu et al., 2015; Wang et al., 2016; Hu, 2009
AT1G58180	β CA6 (Beta Carbonic Anhydrase 6)	Encodes β -carbonic anhydrase 6	Minor role in CO ₂ sensing among carbonic anhydrases	Hu et al., 2010
AT1G62400	HT1 (high leaf temperature 1)	Protein kinase	Key negative regulator of the CO ₂ -induced stomatal response	Hashimoto et al., 2006; H \ddot{o} rak et al., 2016
AT1G62262	SLAH1 (Slac1 Homologue 1)	SLAC1-like anion transporter	Involved in ion homeostasis; plasma membrane localised	Negi et al., 2008
AT1G62280	SLAH4 (Slac1 Homologue 4)	SLAC1-like anion channel in guard cells	Possible role in CO ₂ -induced stomatal conductance via ion regulation, given its similarity to SLAC1	Negi et al., 2008
AT1G75100	JAC1(J-Domain Protein Required for Chloroplast Accumulation Response)	J-domain protein required for chloroplast accumulation and movement	Important for chloroplast movement. Affects stomatal aperture and CO ₂ uptake, and is involved in oxidative stress responses	Czarnocka et al., 2020
AT1G70950	WDL7 (Wave-Dampened2-Like 7)	A microtubule-stabilising protein	Part of microtubule degradation in ABA induced stomatal closure	Dou et al., 2021
AT1G63490	JMJ17 (Jumonji Domain-Containing Protein17)	Histone demethylase	Modulates OST1 expression and thereby affects stomatal closure in the ABA response	Huang et al., 2019
AT1G60490	VPS34 (Vacuolar Protein Sorting34)	Vacuolar protein sorting 34; phosphatidylinositol 3-kinase	Implicated in CO ₂ signaling via phosphoinositide pathways affecting stomatal closure	Takahashi et al., 2017

AT1G 73670	MPK15 (Mito- gen-Activated Protein Ki- nase15)	Mitogen-activated protein kinase	Possible involvement in stress signalling; no di- rect CO ₂ link yet	Kazuya Ichimura et al.,2002
AT1G 59580	MPK2 (Mito- gen-Activated Protein Kinase 2)	Mitogen-activated protein kinase	Stress-activated kinase with possible overlap to ABA signalling	Ortiz-Masia et al., 2007
AT1G 60890	PI4P5Ks (Phosphatidyl- inositol 4- Phosphate 5- Kinases)	Phosphatidylinosi- tol-4-phosphate 5-ki- nase family protein	Associated with integrat- ing environmental and hormonal signals	Lin et al., 2004
AT1G 60940	SnRK2.10 (Snf1-Related Protein Kinase 2.10)	Encodes protein a ki- nases SnRK2	Part of a kinase family involved in abscisic acid (ABA) and CO ₂ medi- ated stress signaling	Wang et al., 2023.
AT1G 57870	SK42 (Shaggy-Like Kinase 42)	A glycogen synthase kinase 3	Involved in diverse stress responses	Li et al., 2021

5 Discussion

This study investigated the genetic basis underlying natural variations in the stomatal response to elevated CO₂ concentration in *A. thaliana* MAGIC RILs. There was considerable variation in the short-term stomatal responses to elevated CO₂ across genotypes in the mapping population, with g_s reductions ranging from 7% to 54%, consistent with earlier studies in *A. thaliana* and other species (Morison, 1998; Haworth et al., 2013; Medlyn et al., 2001). The genetic basis of this variation was explored through QTL mapping, which resulted in the identification of a QTL at the end of chromosome 1. A previous QTL mapping study of stomatal regulation in response to elevated CO₂ by Johansson et al. (2020) reported multiple QTLs on different chromosomes, but none of them overlapped with those found in this study. This suggests that additional loci contribute to natural variation in CO₂ responses, and that further QTLs could potentially be revealed under different experimental conditions or with expanded populations.

A SNP association scan and a gene search within the QTL region revealed 15 candidate genes. Interestingly, the SNP marker that showed strong association with the QTL peak for short-term CO₂-induced % reduction in g_s was linked to the gene FAB1C, located approximately 377 kb downstream of the QTL peak. FAB1C encodes *PI3P5K*, an enzyme involved in the biosynthesis of PI(3,5)P₂, a signalling lipid that contributes to vacuolar acidification, which is essential for guard cell turgor regulation during ABA-induced stomatal closure. Loss-of-function

mutants of *FAB1C* exhibit delayed stomatal responses to ABA, likely due to reduced vacuolar acidification and delay in stomatal closure (Bak et al., 2013). It is known that PI(3,5)P₂, involved in vacuolar acidification, does not directly affect vacuolar proton pumps but instead regulates vacuolar ion channels like *CLC-a* (Chloride Channel A) (Carpaneto et al., 2017). *CLC-a* is a NO³⁻/H⁺ exchanger that contributes to vacuolar ion homeostasis, and its inhibition by PI(3,5)P₂ enhances vacuolar acidification, leading to stomatal closure. Additionally, *CLC-a* is activated by *OST1*, a key kinase involved in both ABA and CO₂ signalling pathways, further linking *FAB1C* activity to stomatal regulation under both conditions. Since the regulation of the *CLC-a* ion exchanger is already influenced by a component shared by both pathways, it underlines the importance of examining the role of PI(3,5)P₂-mediated *CLC-a* regulation in this context (Wege et al., 2014).

Stomatal closure in response to elevated CO₂ converges downstream with the ABA-induced stomatal closure pathway. Current models indicate that CO₂-induced signalling merges with ABA signalling at or upstream of *OST1*, a key kinase that activates the *SLAC1* anion channel and mediates guard cell turgor changes (Mustilli et al., 2002; Fujii et al., 2009). The reduction of guard cell volume during stomatal closure depends on regulation of ion and water fluxes across both plasma and vacuolar membranes (Vahisalu et al., 2008; Mirasole et al., 2023). Notably, recent studies have highlighted the importance of vacuolar membrane regulation in stomatal responses to environmental stimuli such as ABA and CO₂ (Isner et al., 2018; Zhang et al., 2018).

Moving on to the other genes identified from the QTL region, two well-known genes, β CA4 and HT1, both are key components involved in CO₂-induced stomatal closure. β CA4, along with β CA1, plays an early role in CO₂ sensing by converting CO₂ to bicarbonate, which acts as a second messenger in the signalling cascade (Hu et al., 2010). HT1 is a protein kinase that negatively regulates CO₂-induced stomatal closure. It is also part of the broader signalling network that responds to environmental cues (Hashimoto et al., 2006; Hashimoto-Sugimoto et al., 2016; H \ddot{o} rak et al., 2016). Recent studies show that HT1 forms a complex with MAP kinases MPK4 and MPK12, acting as an early bicarbonate sensor in the CO₂-induced pathway. Under high CO₂, β CA1/4 enhances CO₂-to-bicarbonate conversion, triggering MPK4/12 binding to HT1 (H \ddot{o} rak et al., 2016; Jakobson et al., 2016; T \ddot{o} ldsepp et al., 2018; Takahashi et al., 2022). This inhibits HT1 kinase activity, downregulating CBC1 (Convergence of Blue Light and CO₂ 1) kinase and allowing kinases like OST1 and GHR1 to activate the SLAC1 anion channel. This leads to ion efflux from guard cells, resulting in stomatal closure (Vahisalu et al., 2008; Sierla et al., 2018; Hiyama et al., 2017).

In addition to the previously mentioned genes, the region has twelve other candidate genes that are potential targets for further functional analysis. These genes fall into two broad categories: kinases involved in various signal transduction pathways and genes associated with stress responses and the ABA signalling pathway. Because CO₂ and ABA signalling pathways overlap at several points, genes involved in ABA-induced stomatal closure may also contribute to CO₂ responses. Similarly, genes linked to general stress responses may also play a role, warranting further investigation.

Since QTL mapping identifies genomic regions rather than exact causal genes, examining all potential candidates in the interval is important. Functional validation will be necessary to determine the underlying relationship.

During the final stages of analysis, some unusual values were noticed in the data visualisation. After the removal of these outliers, a final round of QTL mapping led to the discovery of an additional QTL associated with half response time. A major portion of the QTL support interval for half-response time overlaps with that of the QTL peak for % reduction in g_s . However, since correlation analysis showed no relationship between these two traits, it suggests they may be controlled by different genes. Alternatively, it remains possible that a shared genetic region could influence both traits through separate mechanisms, or that two closely linked genes may be acting in coordination. Further detailed investigation is needed to clarify these possibilities.

Another noteworthy observation was the weak correlation between g_s and photosynthesis. One possible explanation could be the diverse genetic makeup within the MAGIC population, which was generated through a large number of recombination events. As a next step, it could be valuable to investigate the factors influencing photosynthesis variation more deeply, potentially through mapping photosynthetic capacity or exploring this variance using MAGIC populations.

Interestingly, some genotypes displayed low stomatal conductance alongside relatively high photosynthetic rates. This combination indicates high water use efficiency, implying reduced water loss without compromising carbon assimilation. These genotypes could be promising candidates for further exploration, particularly in mapping *loci* linked to water use efficiency. Investigating this trait could reveal genetic mechanisms that enable plants to optimise gas exchange under elevated CO₂ or water-limiting conditions, which has direct implications for improving crop performance in the face of climate change.

5.1 Next steps

The QTL identified for % reduction in g_s in this study is significant; however, its support interval is quite broad, ranging from 22.94–28.89 Mbp. One possible reason for this could be the limited number of genotypes (206 MAGIC RILs) used in the analysis. While this number is larger than what is generally used in biparental populations, it might still be insufficient considering the complexity and allelic diversity within a MAGIC population. Increasing the number of lines would not just strengthen the power of the analysis but also help narrow down the QTL region by improving mapping precision (Kover et al., 2009; Keele et al., 2019). This is especially important in a highly diverse population like MAGIC, where the frequency of some alleles may be low (Keele et al., 2019). Although replication within lines can reduce environmental noise and improve trait accuracy, it does not increase the proportion of genetic variance a QTL explains. Therefore, adding more genotypes to the QTL analysis is generally more valuable than increasing the number of replicates per line. Even so, replicates of individual lines are useful to reduce background noise and environmental variation, which can improve the quality of the phenotypic data (Kearsey, 1998; Kover et al., 2009; Keele et al., 2019). The decision to prioritise the number of lines over the number of replicates was relevant in this study, as the phenotype being measured is time-consuming and labour-intensive. Therefore, priority was given to increasing the number of lines, rather than replicates, to maximise the power and resolution of QTL detection. One of the immediate steps is to add more samples to the current study by growing more batches of MAGIC lines under similar conditions and make sure the phenotype is consistent across the batches using control lines with each batch.

Another key step is to examine the effect of parental alleles. This will help determine which parents contribute positively, negatively, or neutrally to traits such as the % reduction in stomatal conductance. Once the positive-effect parents are identified, they can be backcrossed

with negative or neutral lines to develop Near Isogenic Lines (NILs). NILs are nearly identical except for the QTL region, which allows for confirmation of the effect of the QTL (Li et al., 2020). A detailed look at allele distribution across the full set of 527 MAGIC RILs (Kover et al., 2009) will also help identify additional lines that carry favourable alleles, which can be prioritised for NIL development or functional studies.

Finally, functional validation of the candidate genes within the QTL interval could be carried out using T-DNA knockout mutants. A T-DNA knockout mutant is a plant line where a specific gene has been disrupted by the insertion of a large DNA fragment (T-DNA) through transformation using the bacterium *Agrobacterium tumefaciens*. This insertion can interrupt the expression of the gene, allowing researchers to study the effects of its loss of function (Sangwan et al., 2012; O'Malley et al., 2015). By comparing the stomatal response of mutants to that of wild-type plants, we can investigate if the gene affects stomatal closure under elevated CO₂. However, since the MAGIC lines have a complex genetic background derived from 19 different parents, any findings from T-DNA mutants, which are usually in the Col-0 background, should be interpreted with care. It may be necessary to consider that some variation may be related to gain-of-function mutations in some parent lines relative to Col-0.

6 Conclusion

This study is an initial step towards investigating genetic components involved in CO₂-induced stomatal closure among a diverse set of Arabidopsis genotypes. While a significant QTL region on chromosome 1 was identified, further research is needed to narrow down the QTL location by increasing the sample size and investigating parental allele effects. Functionals analysis of key candidate genes such as FAB1C, which may play a role in vacuolar regulation during stomatal closure, will also be an important next step. Ultimately, advancing our understanding of the genetic regulation of stomatal conductance at elevated CO₂ levels will bring us closer to developing strategies for improving drought resistance and water-use efficiency in crops, contributing to food security in a future with increasing CO₂ concentrations.

Acknowledgement

This thesis wouldn't have been possible without my supervisor Mats, who trusted me and offered this challenging yet rewarding project. I would like to extend my deepest gratitude to him for all his guidance and constant support. I'm also grateful for his confidence in me, his flexibility, and kindness throughout this journey—I've learned so much both academically and personally.

I'm equally grateful to Karin, who guided me in every step with patience and dedication. Your knowledge and encouragement shaped this project and motivated me deeply. You are truly a great teacher.

My sincere thanks to Diana Laura for her constant help and company, and Kim for showing genuine interest in my project and keeping me company during lonely hours in the phytotron.

Thanks also to my examiner, Henrik, whose support and kind questions whenever we met were an encouragement, especially when he asked with a small smile, “Have you found something?”— I’m happy to say, yes, I finally did!

Finally, my deepest thanks to my husband Tom and my children Daniel and Rachel for their unwavering love, patience, support, and understanding. You are my backbone and greatest strength. I truly could not have done it without you.

References

- Ainsworth, E. A., and Rogers, A. . (2007). The response of photosynthesis and stomatal conductance to rising [CO₂]: mechanisms and environmental interactions. *Plant Cell Environ*, 30, 258–270. <https://doi.org/10.1111/j.1365-3040.2007.01641.x>
- Alonso-Blanco, C., & Koornneef, M. (2000). Naturally occurring variation in Arabidopsis: an underexploited resource for plant genetics. *Trends Plant Sci*, 5(1), 22-29. [https://doi.org/10.1016/s1360-1385\(99\)01510-1](https://doi.org/10.1016/s1360-1385(99)01510-1)
- Asargew, M. F., Masutomi, Y., Kobayashi, K., and Aono, M. (2024). Water stress changes the relationship between photosynthesis and stomatal conductance. *Science of The Total Environment*, 907, 167886. <https://doi.org/https://doi.org/10.1016/j.scitotenv.2023.167886>
- Bahar B, Y. M. and Barutcular C. (2009). Relationships between Stomatal Conductance and Yield Components in Spring Durum Wheat under Mediterranean Conditions. *Notulae Botanicae Horti Agrobotanici Cluj-Napoca*, 37(2), 45–48.
- Bak, G., Lee, E. J., Lee, Y., Kato, M., Segami, S., Sze, H., Maeshima, M., Hwang, J. U. and Lee, Y. (2013). Rapid structural changes and acidification of guard cell vacuoles during stomatal closure require phosphatidylinositol 3,5-bisphosphate. *Plant Cell*, 25(6), 2202-2216. <https://doi.org/10.1105/tpc.113.110411>
- Broman, K. W., Gatti, D. M., Simecek, P., Furlotte, N. A., Prins, P., Sen, Š., Yandell, B. S., and Churchill, G. A. (2019). R/qt2: Software for Mapping Quantitative Trait Loci with High-Dimensional Data and Multiparent Populations. *Genetics*, 211(2), 495-502. <https://doi.org/10.1534/genetics.118.301595>
- Carpaneto, A., Boccaccio, A., Lagostena, L., Di Zanni, E., and Scholz-Starke, J. (2017). The signaling lipid phosphatidylinositol-3,5-bisphosphate targets plant CLC-a anion/H⁺ exchange activity. *EMBO reports*, 18(7), 1100-1107. <https://doi.org/https://doi.org/10.15252/embr.201643814>
- Cavanagh, C., Morell, M., Mackay, I., and Powell, W. (2008). From mutations to MAGIC: resources for gene discovery, validation and delivery in crop plants. *Curr Opin Plant Biol*, 11(2), 215-221. <https://doi.org/10.1016/j.pbi.2008.01.002>
- Churchill G A, D. R. W. (1994). Empirical threshold values for quantitative trait mapping.

Genetics 138, 963–971.

- Czarnocka, W., Rusaczonek, A., Willems, P., Sujkowska-Rybkowska, M., Van Breusegem, F., and Karpiński, S. (2020). Novel Role of JAC1 in Influencing Photosynthesis, Stomatal Conductance, and Photooxidative Stress Signalling Pathway in *Arabidopsis thaliana*. *Front Plant Sci*, 11, 1124. <https://doi.org/10.3389/fpls.2020.01124>
- Dou, L., He, K., Peng, J., Wang, X., and Mao, T. (2021). The E3 ligase MREL57 modulates microtubule stability and stomatal closure in response to ABA. *Nature Communications*, 12(1), 2181. <https://doi.org/10.1038/s41467-021-22455-y>
- Driesen, E., Van den Ende, W., De Proft, M., and Saeys, W. (2020). Influence of Environmental Factors Light, CO₂, Temperature, and Relative Humidity on Stomatal Opening and Development: A Review. *Agronomy*, 10(12), 1975. <https://www.mdpi.com/2073-4395/10/12/1975>
- Falconer, D. S. a. M., and T.F.C. (1996). *Introduction to Quantitative Genetics* (4th Edition ed.). Addison Wesley Longman.
- Fourquet, L., Barber, T., Campos-Mantello, C., Howell, P., Orman-Ligeza, B., Percival-Alwyn, L., Rose, G. A., Sheehan, H., Wright, T. I. C., Longin, F., Würschum, T., Novoselovic, D., Greenland, A. J., Mackay, I. J., Cockram, J., and Bentley, A. R. (2024). An eight-founder wheat MAGIC population allows fine-mapping of flowering time loci and provides novel insights into the genetic control of flowering time. *Theor Appl Genet*, 137(12), 277. <https://doi.org/10.1007/s00122-024-04787-7>
- Fujii, H., Chinnusamy, V., Rodrigues, A., Rubio, S., Antoni, R., Park, S. Y., Cutler, S. R., Sheen, J., Rodriguez, P. L., and Zhu, J. K. (2009). In vitro reconstitution of an abscisic acid signalling pathway. *Nature*, 462(7273), 660-664. <https://doi.org/10.1038/nature08599>
- Haley, C. S. and Knott., S. A. (1992). A simple regression method for mapping quantitative trait loci in line crosses using flanking markers. *Heredity*, 69, 315–324.
- Hashimoto, M., Negi, J., Young, J., Israelsson, M., Schroeder, J. I., and Iba, K. (2006). *Arabidopsis* HT1 kinase controls stomatal movements in response to CO₂. *Nat Cell Biol*, 8(4), 391-397. <https://doi.org/10.1038/ncb1387>
- Hashimoto-Sugimoto, M., Negi, J., Monda, K., Higaki, T., Isogai, Y., Nakano, T., Hasezawa, S., and Iba, K. (2016). Dominant and recessive mutations in the Raf-like kinase HT1 gene completely disrupt stomatal responses to CO₂ in *Arabidopsis*. *J Exp Bot*, 67(11), 3251-3261. <https://doi.org/10.1093/jxb/erw134>
- Hasper TB, D. M., Breuer F, Uwizeye FK, Wallin G and Uddling J. (2017). Stomatal CO₂ responsiveness and photosynthetic capacity of tropical woody species in relation to taxonomy and functional traits. *Oecologia*, 184, 43–57
- Hatfield, J., Boote, K., Kimball, B. A., Ziska, L., Izaurralde, R., Ort, D., and Thomson, A. (2011). Climate Impacts on Agriculture: Implications for Crop Production. *Agronomy Journal*, 103, 351-370. <https://doi.org/10.2134/agronj2010.0303>

- Haworth, M., Elliott-Kingston, C., and McElwain, J. (2013). Haworth, M., Elliott-Kingston, C., McElwain, J.C. (2013) Co-ordination of physiological and morphological responses of stomata to elevated [CO₂] in vascular plants. *Oecologia* 171(1):71-82. *Oecologia*, 171, 71-82
- He, J., Zhang, R. X., Peng, K., Tagliavia, C., Li, S., Xue, S., Liu, A., Hu, H., Zhang, J., Hubbard, K. E., Held, K., McAinsh, M. R., Gray, J. E., Kudla, J., Schroeder, J. I., Liang, Y. K., and Hetherington, A. M. (2018). The BIG protein distinguishes the process of CO₂-induced stomatal closure from the inhibition of stomatal opening by CO₂. *New Phytol*, 218(1), 232-241. <https://doi.org/10.1111/nph.14957>
- Hetherington, A. M., and Woodward, F. I. . (2003). The role of stomata in sensing and driving environmental change. *Nature*, 424(6951), 901-908.
- Hiyama, A., Takemiya, A., Munemasa, S., Okuma, E., Sugiyama, N., Tada, Y., Murata, Y., and Shimazaki, K.-i. (2017). Blue light and CO₂ signals converge to regulate light-induced stomatal opening. *Nature Communications*, 8(1), 1284. <https://doi.org/10.1038/s41467-017-01237-5>
- Holland, J. B. (2007). Genetic architecture of complex traits in plants. *Current Opinion in Plant Biology*, 10(2), 156-161. <https://doi.org/https://doi.org/10.1016/j.pbi.2007.01.003>
- Hörak, H., Sierla, M., Töldsepp, K., Wang, C., Wang, Y.-S., Nuhkat, M., Valk, E., Pechter, P., Merilo, E., Salojärvi, J., Overmyer, K., Loog, M., Brosché, M., Schroeder, J. I., Kangasjärvi, J., and Kollist, H. (2016). A Dominant Mutation in the HT1 Kinase Uncovers Roles of MAP Kinases and GHR1 in CO₂-Induced Stomatal Closure. *The Plant Cell*, 28(10), 2493-2509. <https://doi.org/10.1105/tpc.16.00131>
- Hsu, P.-K., Takahashi, Y., Munemasa, S., Merilo, E., Laanemets, K., Waadt, R., Pater, D., Kollist, H., and Schroeder, J. I. (2018). Abscisic acid-independent stomatal CO₂ signal transduction pathway and convergence of CO₂ and ABA signaling downstream of OST1 kinase. *Proceedings of the National Academy of Sciences*, 115(42), E9971-E9980. <https://doi.org/doi:10.1073/pnas.1809204115>
- Hu, H., Boisson-Dernier, A., Israelsson-Nordström, M., Böhmer, M., Xue, S., Ries, A., Godoski, J., Kuhn, J. M., and Schroeder, J. I. (2010). Carbonic anhydrases are upstream regulators of CO₂-controlled stomatal movements in guard cells. *Nat Cell Biol*, 12(1), 87-93; sup pp 81-18. <https://doi.org/10.1038/ncb2009>
- Huang, S., Zhang, A., Jin, J. B., Zhao, B., Wang, T.-J., Wu, Y., Wang, S., Liu, Y., Wang, J., Guo, P., Ahmad, R., Liu, B., and Xu, Z.-Y. (2019). Arabidopsis histone H3K4 demethylase JM17 functions in dehydration stress response. *New Phytologist*, 223(3), 1372-1387. <https://doi.org/https://doi.org/10.1111/nph.15874>
- Huang, X., Feng, Q., Qian, Q., Zhao, Q., Wang, L., Wang, A., Guan, J., Fan, D., Weng, Q., Huang, T., Dong, G., Sang, T., and Han, B. (2009). High-throughput genotyping by whole-genome resequencing. *Genome Res*, 19(6), 1068-1076. <https://doi.org/10.1101/gr.089516.108>

- Huang, X., Paulo, M. J., Boer, M., Effgen, S., Keizer, P., Koornneef, M., & van Eeuwijk, F. A. (2011). Analysis of natural allelic variation in *Arabidopsis* using a multiparent recombinant inbred line population. *Proc Natl Acad Sci U S A*, *108*(11), 4488-4493. <https://doi.org/10.1073/pnas.1100465108>
- Klein T, Ramon U. Stomatal sensitivity to CO₂ diverges between angiosperm and gymnosperm tree species. *Funct Ecol*. 2019; 33: 1411–1424. <https://doi.org/10.1111/1365-2435.13379>
- LI-COR Biosciences Inc. (2011). *Using the LI6400/LI6400XT portable photosynthesis system*. Lincoln, NE: LI-COR Biosciences
- Isner, J. C., Begum, A., Nuehse, T., Hetherington, A. M., & Maathuis, F. J. M. (2018). KIN7 Kinase Regulates the Vacuolar TPK1 K(+) Channel during Stomatal Closure. *Curr Biol*, *28*(3), 466-472.e464. <https://doi.org/10.1016/j.cub.2017.12.046>
- López-Ruiz, B.A, Joshua Banta, Perla Salazar-Hernández et al. QTL mapping using *Arabidopsis thaliana* MAGIC Lines identifies candidate genes controlling adventitious root development, 30 May 2024, PREPRINT (Version 1) available at Research Square [<https://doi.org/10.21203/rs.3.rs-4432917/v1>]
- Izumi C. Mori, J. R., Mineo Shibasaka, Shizuka Sasano, Toshiyuki Kaneko, Tomoaki Horie and Maki Katsuhara. (2014). CO₂ transport by PIP2 aquaporins of barley. *Plant and Cell Physiology*, *55*(2). <https://doi.org/10.1093/pcp/pcu003>
- Jakobson, L., Vaahtera, L., Töldsepp, K., Nuhkat, M., Wang, C., Wang, Y. S., Hōrak, H., Valk, E., Pechter, P., Sindarovska, Y., Tang, J., Xiao, C., Xu, Y., Gerst Talas, U., García-Sosa, A. T., Kangasjärvi, S., Maran, U., Remm, M., Roelfsema, M. R., and Brosché, M. (2016). Natural Variation in *Arabidopsis Cvi-0* Accession Reveals an Important Role of MPK12 in Guard Cell CO₂ Signaling. *PLoS Biol*, *14*(12), e2000322. <https://doi.org/10.1371/journal.pbio.2000322>
- Johansson, K. S. L., El-Soda, M., Pagel, E., Meyer, R. C., Töldsepp, K., Nilsson, A. K., Brosché, M., Kollist, H., Uddling, J., and Andersson, M. X. (2020). Genetic controls of short- and long-term stomatal CO₂ responses in *Arabidopsis thaliana*. *Ann Bot*, *126*(1), 179-190. <https://doi.org/10.1093/aob/mcaa065>
- Karl W. Broman , S. S. (2009). *A Guide to QTL Mapping with R/qtl* (1 ed.). Springer New York. <https://doi.org/https://doi.org/10.1007/978-0-387-92125-9>
- Kearsey, M. J. (1998). The principles of QTL analysis (a minimal mathematics approach). *Journal of Experimental Botany*, *49*(327), 1619-1623. <https://doi.org/10.1093/jxb/49.327.1619>
- Keele, G. R., Crouse, W. L., Kelada, S. N. P., and Valdar, W. (2019). Determinants of QTL Mapping Power in the Realized Collaborative Cross. *G3 Genes|Genomes|Genetics*, *9*(5), 1707-1727. <https://doi.org/10.1534/g3.119.400194>
- Kim, T. H., Böhmer, M., Hu, H., Nishimura, N., and Schroeder, J. I. (2010). Guard cell signal

- transduction network: advances in understanding abscisic acid, CO₂, and Ca²⁺ signaling. *Annu Rev Plant Biol*, 61, 561-591. <https://doi.org/10.1146/annurev-arplant-042809-112226>
- Kollist, H., Nuhkat, M., and Roelfsema, M. R. G. (2014). Closing gaps: linking elements that control stomatal movement. *New Phytologist*, 203(1), 44-62. <https://doi.org/https://doi.org/10.1111/nph.12832>
- Korte, A., and Farlow, A. (2013). The advantages and limitations of trait analysis with GWAS: a review. *Plant Methods*, 9(1), 29. <https://doi.org/10.1186/1746-4811-9-29>
- Kover, P. X., and Schaal, B. A. (2002). Genetic variation for disease resistance and tolerance among *Arabidopsis thaliana* accessions. *Proc Natl Acad Sci U S A*, 99(17), 11270-11274. <https://doi.org/10.1073/pnas.102288999>
- Lander, E. S., and Botstein, D. (1989). Mapping mendelian factors underlying quantitative traits using RFLP linkage maps. *Genetics*, 121(1), 185-199. <https://doi.org/10.1093/genetics/121.1.185>
- Lawson T, B. M. (2014). Stomatal Size, Speed, and Responsiveness Impact on Photosynthesis and Water Use Efficiency. . *Plant Physiology* 164, 1556-1570.
- Lin, W. H., Ye, R., Ma, H., Xu, Z. H., and Xue, H. W. (2004). DNA chip-based expression profile analysis indicates involvement of the phosphatidylinositol signaling pathway in multiple plant responses to hormone and abiotic treatments. *Cell Res*, 14(1), 34-45. <https://doi.org/10.1038/sj.cr.7290200>
- Lu, L., Liu, H., Wu, Y., and Yan, G. (2020). Development and Characterization of Near-Iso-genic Lines Revealing Candidate Genes for a Major 7AL QTL Responsible for Heat Tolerance in Wheat [Original Research]. *Frontiers in Plant Science, Volume 11 - 2020*. <https://doi.org/10.3389/fpls.2020.01316>
- Lu, Z., Percy R. G., Qualset C. O, and Zeiger E., . (1998). Stomatal conductance predicts yields in irrigated Pima cotton and bread wheat grown at high temperatures. *Journal of Experimental Botany*, 49, 453–460.
- Mackay, I. J., Bansept-Basler, P., Barber, T., Bentley, A. R., Cockram, J., Gosman, N., Greenland, A. J., Horsnell, R., Howells, R., O'Sullivan, D. M., Rose, G. A., and Howell, P. J. (2014). An eight-parent multiparent advanced generation inter-cross population for winter-sown wheat: creation, properties, and validation. *G3 (Bethesda)*, 4(9), 1603-1610. <https://doi.org/10.1534/g3.114.012963>
- Medlyn, B. E., Barton, C. V. M., Broadmeadow, M. S. J., Ceulemans, R., De Angelis, P., Forstreuter, M., Freeman, M., Jackson, S. B., Kellomäki, S., Laitat, E., Rey, A., Roberntz, P., Sigurdsson, B. D., Strassmeyer, J., Wang, K., Curtis, P. S., and Jarvis, P. G. (2001). Stomatal conductance of forest species after long-term exposure to elevated CO₂ concentration: a synthesis. . *New Phytologist* 149., 247–264.
- Mirasole, F. M., Nastasi, S. P., Cubero-Font, P., and De Angeli, A. (2023). Vacuolar control of stomatal opening revealed by 3D imaging of the guard cells. *Scientific Reports*,

13(1), 7647. <https://doi.org/10.1038/s41598-023-34273-x>

- Monda, K., Araki, H., Kuhara, S., Ishigaki, G., Akashi, R., Negi, J., Kojima, M., Sakakibara, H., Takahashi, S., Hashimoto-Sugimoto, M., Goto, N., and Iba, K. (2016). Enhanced Stomatal Conductance by a Spontaneous Arabidopsis Tetraploid, Me-0, Results from Increased Stomatal Size and Greater Stomatal Aperture *Plant Physiology*, 170(3), 1435-1444. <https://doi.org/10.1104/pp.15.01450>
- Morison, J. I. L. (1998). Stomatal response to increased CO₂ concentration. *Journal of Experimental Botany*, 49(Special_Issue), 443-452. https://doi.org/10.1093/jxb/49.Special_Issue.443
- Mustilli, A. C., Merlot, S., Vavasseur, A., Fenzi, F., & Giraudat, J. (2002). Arabidopsis OST1 protein kinase mediates the regulation of stomatal aperture by abscisic acid and acts upstream of reactive oxygen species production. *Plant Cell*, 14(12), 3089-3099. <https://doi.org/10.1105/tpc.007906>
- Myles, S., Peiffer, J., Brown, P. J., Ersoz, E. S., Zhang, Z., Costich, D. E., & Buckler, E. S. (2009). Association mapping: critical considerations shift from genotyping to experimental design. *Plant Cell*, 21(8), 2194-2202. <https://doi.org/10.1105/tpc.109.068437>
- NASC. *European Arabidopsis Stock Centre* <https://arabidopsis.info/>
- Negi, J., Matsuda, O., Nagasawa, T., Oba, Y., Takahashi, H., Kawai-Yamada, M., Uchimiya, H., Hashimoto, M., and Iba, K. (2008). CO₂ regulator SLAC1 and its homologues are essential for anion homeostasis in plant cells. *Nature*, 452(7186), 483-486. <https://doi.org/10.1038/nature06720>
- O'Malley, R. C., Barragan, C. C., and Ecker, J. R. (2015). A user's guide to the Arabidopsis T-DNA insertion mutant collections. *Methods Mol Biol*, 1284, 323-342. https://doi.org/10.1007/978-1-4939-2444-8_16
- Ooka, H., Satoh, K., Doi, K., Nagata, T., Otomo, Y., Murakami, K., Matsubara, K., Osato, N., Kawai, J., Carninci, P., Hayashizaki, Y., Suzuki, K., Kojima, K., Takahara, Y., Yamamoto, K., and Kikuchi, S. (2003). Comprehensive analysis of NAC family genes in *Oryza sativa* and *Arabidopsis thaliana*. *DNA Res*, 10(6), 239-247. <https://doi.org/10.1093/dnares/10.6.239>
- Ortiz-Masia, D., Perez-Amador, M. A., Carbonell, J., and Marcote, M. J. (2007). Diverse stress signals activate the C1 subgroup MAP kinases of Arabidopsis. *FEBS Lett*, 581(9), 1834-1840. <https://doi.org/10.1016/j.febslet.2007.03.075>
- Felipe Klein Ricachenevsky, Ana Carolina A L Campos, Paloma Koprovski Menguer, Fernando Mateus Michelon Betin, Jaime Tovar, William F A van Dijk, Mary Lou Guerinot, David E Salt and Paula X Kover, Comparison of linkage and association mapping in MAGIC lines identifies *AtMTP3* as a new gene controlling natural variation in leaf zinc concentration in Arabidopsis, *Journal of Experimental Botany*, 2025;; eraf142, <https://doi.org/10.1093/jxb/eraf142>
- Roux, B., and Leonhardt, N. (2018). Chapter Seven - The Regulation of Ion Channels and

- Transporters in the Guard Cell. In C. Maurel (Ed.), *Advances in Botanical Research* (Vol. 87, pp. 171-214). Academic Press. <https://doi.org/https://doi.org/10.1016/bs.abr.2018.09.013>
- Sangwana R. S. , Sergio Ochattb, José-Edmundo Nava-Saucedo and Brigitte Sangwan-Norreela. (2012). *T-DNA Insertion Mutagenesis*. Retrieved 18-05-2025 from <https://www.researchgate.net/publication/287539411>
- Schneider CA, R. W., and Eliceiri KW. (2012). NIH Image to ImageJ: 25 years of image analysis. *Nature Methods* 9, 671–675.
- Scott, M. F., Ladejobi, O., Amer, S., Bentley, A. R., Biernaskie, J., Boden, S. A., Clark, M., Dell'Acqua, M., Dixon, L. E., Filippi, C. V., Fradgley, N., Gardner, K. A., Mackay, I. J., O'Sullivan, D., Percival-Alwyn, L., Roorkiwal, M., Singh, R. K., Thudi, M., Varshney, and R. K., Mott, R. (2020). Multi-parent populations in crops: a toolbox integrating genomics and genetic mapping with breeding. *Heredity*, 125(6), 396-416. <https://doi.org/10.1038/s41437-020-0336-6>
- Sierla, M., Hörak, H., Overmyer, K., Waszczak, C., Yarmolinsky, D., Maierhofer, T., Vainonen, J. P., Salojärvi, J., Denessiouk, K., Laanemets, K., Töldsepp, K., Vahisalu, T., Gauthier, A., Puukko, T., Paulin, L., Auvinen, P., Geiger, D., Hedrich, R., Kollist, H., and Kangasjärvi, J. (2018). The Receptor-like Pseudokinase GHR1 Is Required for Stomatal Closure. *The Plant Cell*, 30(11), 2813-2837. <https://doi.org/10.1105/tpc.18.00441>
- Somerville, C., & Koornneef, M. (2002). A fortunate choice: the history of Arabidopsis as a model plant. *Nat Rev Genet*, 3(11), 883-889. <https://doi.org/10.1038/nrg927>
- Song, Y., Wang, Y., Yu, Q., Sun, Y., Zhang, J., Zhan, J., and Ren, M. (2023). Regulatory network of GSK3-like kinases and their role in plant stress response. *Front Plant Sci*, 14, 1123436. <https://doi.org/10.3389/fpls.2023.1123436>
- Stadlmeier, M., Hartl, L., and Mohler, V. (2018). Usefulness of a Multiparent Advanced Generation Intercross Population With a Greatly Reduced Mating Design for Genetic Studies in Winter Wheat [Original Research]. *Frontiers in Plant Science*, 9. <https://doi.org/10.3389/fpls.2018.01825>
- Stracke, S., Sato, S., Sandal, N., Koyama, M., Kaneko, T., Tabata, S., and Parniske, M. (2004). Exploitation of colinear relationships between the genomes of *Lotus japonicus*, *Pisum sativum* and *Arabidopsis thaliana*, for positional cloning of a legume symbiosis gene. *Theor Appl Genet*, 108(3), 442-449. <https://doi.org/10.1007/s00122-003-1438-2>
- TAIR, The Arabidopsis Information Center. <https://www.arabidopsis.org/>
- Takahashi, S., Monda, K., Higaki, T., Hashimoto-Sugimoto, M., Negi, J., Hasezawa, S., and Iba, K. (2017). Differential Effects of Phosphatidylinositol 4-Kinase (PI4K) and 3-Kinase (PI3K) Inhibitors on Stomatal Responses to Environmental Signals. *Front Plant Sci*, 8, 677. <https://doi.org/10.3389/fpls.2017.00677>
- Takahashi, S., Monda, K., Negi, J., Konishi, F., Ishikawa, S., Hashimoto-Sugimoto, M., Goto,

- N., and Iba, K. (2015). Natural variation in stomatal responses to environmental changes among *Arabidopsis thaliana* ecotypes. *PloS one*, *10*(2), e0117449. <https://doi.org/10.1371/journal.pone.0117449>
- Takahashi, Y., Bosmans, K. C., Hsu, P.-K., Paul, K., Seitz, C., Yeh, C.-Y., Wang, Y.-S., Yarmolinsky, D., Sierla, M., Vahisalu, T., Waszczak, C., McCammon, J. A., Kangasjärvi, J., Zhang, L., Kollist, H., Trac, T., and Schroeder, J. I. (2022). Stomatal CO₂/bicarbonate sensor consists of two interacting protein kinases, Raf-like HT1 and non-kinase-activity requiring MPK12/MPK4. *Science Advances*, *8*(49), eabq6161. <https://doi.org/doi:10.1126/sciadv.abq6161>
- Töldsepp, K., Zhang, J., Takahashi, Y., Sindarovska, Y., Hõrak, H., Ceciliato, P. H. O., Koolmeister, K., Wang, Y. S., Vaahtera, L., Jakobson, L., Yeh, C. Y., Park, J., Brosche, M., Kollist, H., and Schroeder, J. I. (2018). Mitogen-activated protein kinases MPK4 and MPK12 are key components mediating CO₂-induced stomatal movements. *Plant J*, *96*(5), 1018-1035. <https://doi.org/10.1111/tpj.14087>
- Vahisalu, T., Kollist, H., Wang, Y. F., Nishimura, N., Chan, W. Y., Valerio, G., Lamminmäki, A., Brosché, M., Moldau, H., Desikan, R., Schroeder, J. I., and Kangasjärvi, J. (2008). SLAC1 is required for plant guard cell S-type anion channel function in stomatal signalling. *Nature*, *452*(7186), 487-491. <https://doi.org/10.1038/nature06608>
- Vilhjálmsón, B. J., and Nordborg, M. (2013). The nature of confounding in genome-wide association studies. *Nat Rev Genet*, *14*(1), 1-2. <https://doi.org/10.1038/nrg3382>
- Wang, H., Wang, Y., Sang, T., Lin, Z., Li, R., Ren, W., Shen, X., Zhao, B., Wang, X., Zhang, X., Zhou, S., Dai, S., Hu, H., Song, C. P., and Wang, P. (2023). Cell type-specific proteomics uncovers a RAF15-SnRK2.6/OST1 kinase cascade in guard cells. *J Integr Plant Biol*, *65*(9), 2122-2137. <https://doi.org/10.1111/jipb.13536>
- Wege, S., De Angeli, A., Droillard, M. J., Kroniewicz, L., Merlot, S., Cornu, D., Gambale, F., Martinoia, E., Barbier-Brygoo, H., Thomine, S., Leonhardt, N., and Filleur, S. (2014). Phosphorylation of the vacuolar anion exchanger AtCLCa is required for the stomatal response to abscisic acid. *Sci Signal*, *7*(333), ra65. <https://doi.org/10.1126/scisignal.2005140>
- Wickham, H. (2016). *ggplot2: Elegant Graphics for Data Analysis* (second edition ed.). Springer-Verlag. https://doi.org/10.1007/978-3-319-24277-4_9
- Xu, S. (2013). Interval Mapping. In S. Xu (Ed.), *Principles of Statistical Genomics* (pp. 109-129). Springer New York. https://doi.org/10.1007/978-0-387-70807-2_9
- Xu, Y., Li, P., Yang, Z., and Xu, C. (2017). Genetic mapping of quantitative trait loci in crops. *The Crop Journal*, *5*(2), 175-184. <https://doi.org/https://doi.org/10.1016/j.cj.2016.06.003>
- Xu Z, J. Y., Jia B and ZhouG. (2016). Elevated-CO₂ Response of Stomata and Its Dependence on Environmental Factors. *Front. Plant Sci.*, *7*, 657. <https://doi.org/doi:10.3389/fpls.2016.00657>

- Xue, S., Hu, H., Ries, A., Merilo, E., Kollist, H., and Schroeder, J. I. (2011). Central functions of bicarbonate in S-type anion channel activation and OST1 protein kinase in CO₂ signal transduction in guard cell. *The EMBO Journal*, 30(8), 1645-1658. <https://doi.org/https://doi.org/10.1038/emboj.2011.68>
- Zinta, G., Abdelgawad, H., Domagalska, M. A., Vergauwen, L., Knapen, D., Nijs, I., Janssens, I. A., Beemster, G. T., and Asard, H. (2014). Physiological, biochemical, and genome-wide transcriptional analysis reveals that elevated CO₂ mitigates the impact of combined heat wave and drought stress in *Arabidopsis thaliana* at multiple organizational levels. *Glob Chang Biol*, 20(12), 3670-3685. <https://doi.org/10.1111/gcb.12626>

Appendix 1

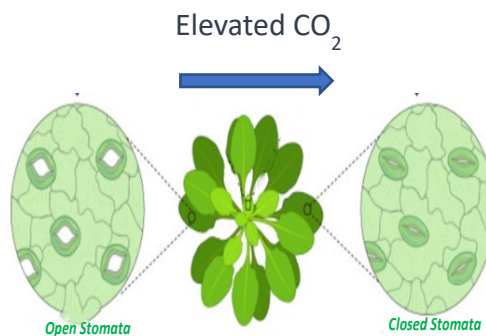
Popular science summary

How plants adapt in a CO₂-increasing world: connecting the genetic puzzle

Did you know that stomata—the tiny breathing pores on the surface of plant leaves—are changing their behaviour in response to climate change? These shifts could reshape agriculture, water use, and food security in the future.

Stomata: small openings, big impact

As carbon dioxide (CO₂) in the atmosphere continues to rise, plants are already starting to respond. One of the key changes happens in their leaves, specifically in the tiny pores called stomata. These act like gatekeepers: they open to let CO₂ in for photosynthesis and release oxygen and water vapour through transpiration. Under elevated CO₂, many plants don't need to open their stomata fully because they get sufficient CO₂ to perform normal photosynthesis. With smaller openings, plants lose less water while still maintaining normal growth and productivity. The degree of this stomatal opening is quantified by stomatal conductance (g_s), which measures the rate of gas exchange through the stomata. Studies have shown that elevated CO₂ can reduce stomatal conductance by approximately 5–60% in many plant species, depending on genotype, growth conditions, and developmental stage. This may sound like a small adjustment, but in a drier, more water-limited future, it could make a big difference for plant survival—and for the crops we rely on.



Under elevated CO₂, plants close these stomata to conserve water—an adaptive shift in a changing climate

So, how do plants actually "know" when to close their stomata as CO₂ levels rise? What are the genetic components that detect and transmit this signal inside the guard cells, the specialised cells that control stomatal opening and closing?

We know this response isn't regulated by a single gene, but rather by a complex signalling network involving multiple genetic components. Some of the key elements have already been identified, but the full picture is still far from complete.

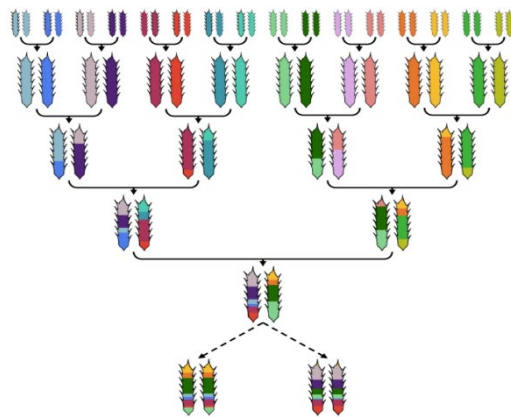
Looking for missing components

In this study, we searched to find some of those missing or connecting pieces in the genetic puzzle. To achieve this, we utilised the MAGIC (Multiparent Advanced Generation Inter-Cross) population of *Arabidopsis thaliana*. These plants carry a rich mix of genes from different parent plants, making them ideal for genetic studies.

We studied the stomatal conductance response in MAGIC of *Arabidopsis* plants grown under controlled conditions. For each plant, we first measured stomatal conductance at ambient CO₂ (420 ppm) until steady-state was reached. Then, we raised the CO₂ to 800 ppm and recorded g_s again to assess the short-term response (response shown within minutes to hours). We calculated the percentage reduction in g_s to quantify how each plant reacted to elevated CO₂. Using this response data, we scanned the plants' chromosomes with a genetic mapping tool to identify DNA regions strongly linked to this stomatal behaviour.

Did you know..

The MAGIC population of Arabidopsis thaliana is created by crossing 19 different parent plants. Each offspring is a unique mix of all those parents. Scientists can more easily zoom in to exact bits of DNA linked to important traits-like how plants respond to rising CO₂. Figure showing an example of the MAGIC cross with 8 parents



A clue on chromosome 1

What we found was a promising QTL (Quantitative Trait Locus) at the end of chromosome 1. A QTL is a region on the chromosome where we can look for genes that might be linked to a measurable trait—in this case, the stomatal response to elevated CO₂. This QTL represents a promising target for further investigation. We have also shortlisted approximately 15 genes that may be functionally linked to the trait from the QTL region. These genes represent potential regulators of the stomatal response to high CO₂ and may include previously unidentified components of the underlying signalling network.

Why these matters

As droughts become more common and CO₂ levels continue to rise, helping crops use water more efficiently is more important than ever. One way plants manage this is by partially closing their stomata under high CO₂, saving water while maintaining productivity. Identifying the genetic regions behind this response is the first step toward discovering the specific genes involved. This knowledge lays the foundation for plant breeders to develop new crop varieties, selecting the best-performing traits to build crops better adapted to a hotter, drier, CO₂-rich future.